

Ultra Wideband Omnidirectional Discone
Antenna for WLAN Applications

Mengchu Wang

Delft University of Technology

Ultra wideband Omnidirectional Discone Antenna for WLAN Applications

By

Mengchu Wang

in partial fulfilment of the requirements for the degree of

Master of Science

in Engineering, Mathematics and Computer Science

at the Delft University of Technology,
to be defended publicly on June 15, 2015 at 11:00 AM.

Thesis advisor:	Prof. DSc. Alexander Yarovoy,
Supervisor:	Ir. Dinh Tran
Thesis committee:	Dr.ir. Gerard Janssen

This thesis is confidential and cannot be made public until June 15, 2016.

An electronic version of this thesis is available at <http://repository.tudelft.nl/>.



Abstract

In the past decade wireless communication was an area of rapid developments. Constant demand to increase the data rate results in an increase of both the number of operational bands in use and the bandwidth within each band. This development requires constant improvement of the front-ends including antennas. The generic trend is to replace single band antennas to multi-band ones or wideband ones. The demands from the market require a new generation of antennas with wideband operation, wide signal coverage, compact dimensions, and lower manufacturing cost.

The focus of this thesis is to design a dielectric covered disccone WLAN antenna working under the protocols of IEEE802.11 a/b/g/n. It has the wideband operation of disccone antennas and the compact dimensions of dielectric resonator antennas which is compatible with the latest main protocol WLAN applications. This antenna has an ultra-wide bandwidth (2.25 GHz-6.0 GHz), which is sufficient for the data communication protocols of IEEE802.11 a/b/g/n (2401 MHz-2484 MHz and 5150 MHz-5825 MHz). Its directivity is 3.1 dBi at the lower frequency band and 5.3 dBi at the higher frequency band, which is enough to cover conventional indoor usages. In order to use similar radiation patterns at both operational bands the quad slot is added to the disk. The antenna is quite competitive compared to other commercially used antennas because of its wideband potential: it can be used not only in WLAN applications, but also for other ultra-wideband applications.

Content

Abstract.....	V
1 Introduction.....	1
1.1 Background of the Research	1
1.2 Objectives	1
1.3 Challenges	3
1.4 Approaches	4
1.5 Novelties	5
1.6 Thesis Outline.....	5
2 State of The Art in WLAN Antennas	7
2.1 Introduction	7
2.2 MIMO Antenna Systems	7
2.3 Planar Inverted F-Antennas (PIFA)	8
2.4 Dielectric Resonator Antennas	9
2.5 Dipole Antennas	11
2.6 Bow-tie Antennas.....	12
2.7 Conical Antennas.....	13
2.7.1 Biconical Antennas.....	13
2.7.2 Discone Antennas	16
2.8 Conclusion.....	18
3 Numerical Analysis of the Dielectric Filled Discone Antenna.....	20
3.1 Introduction	20
3.2 Overview of the Design	20

3.3 Optimization Procedure.....	22
3.3.1 Analysis of Waveguide Cavity	23
3.3.2 Choice of Dielectric Material.....	27
3.3.3 Choice of Feeding method.....	28
3.3.4 Optimization of Cone.....	31
3.3.5 Optimization of Disc	33
3.3.6 Optimization of Ground Plane Radius	35
3.4 Discussion of Antenna Performance	36
4 Dielectric Filled Discone Antenna with Quad Slot	40
4.1 Introduction	40
4.2 Study of Circular Ring Slot Architecture.....	41
4.3 Study of Dual Slot Architecture.....	45
4.4 Study of Quad Slot Architecture	52
5 Conclusions and Recommendations	60
Appendix A.....	62
Appendix B.....	64
Acknowledgements.....	66
Bibliography.....	68

List of Figures

Figure 2.1 Configuration of the six-loop-antenna MIMO system [6]	7
Figure 2.2 Geometries of PIFA antenna [9].....	8
Figure 2.3 Typical dielectric resonator antenna and feeding mechanisms [14]	10
Figure 2.4 Geometry and detailed dimensions of a 2.4/5.2 GHz dual-WLAN unequal-arms dipole antenna [20].....	11
Figure 2.5 The bow-tie antenna.....	12
Figure 2.6 The biconical antenna	14
Figure 2.7 Electric and magnetic fields, and associated voltages and currents, for a biconical antenna.....	15
Figure 2.8 Dielectric covered conical antenna	15
Figure 2.9 Normalized pattern of discone antenna [31].....	17
Figure 3.1 Discone antenna filled with dielectric material.....	21
Figure 3.2 Proposed cavity models	23
Figure 3.3 Rectangular Waveguide Cavity resonators.....	23
Figure 3.4 Cut plane of the square waveguide	24
Figure 3.5 A cylindrical resonant cavity	26
Figure 3.6 The coaxial cable.....	29
Figure 3.7 Semi-rigid cables	30
Figure 3.8 Geometry of the RG402/U coaxial cable	31
Figure 3.9 Optimization of the cone height.....	32
Figure 3.10 Optimization of the cone radius.....	33
Figure 3.11 Optimization of discone overall height.....	34
Figure 3.12 Optimization of disc radius	34
Figure 3.13 Optimization of ground plane radius.....	35
Figure 3.14 Variation of polar radiation patterns in terms of the different ground plane radius	36
Figure 3.15 S11 parameters of the proposed antenna	37
Figure 3.16 Polar radiation patterns of proposed antenna at 2.45 GHz and 5.5 GHz.....	37

Figure 4.1 Electric and magnetic fields, and associated voltages and currents, for a discone antenna.....	41
Figure 4.2 The circular ring slot architecture.....	42
Figure 4.3 Variation of reflection coefficients with slot radius R_1	43
Figure 4.4 Variation of radiation patterns with slot radius at 2.45 GHz and 5.5 GHz.....	43
Figure 4.5 Variation of reflection coefficients with slot width.....	44
Figure 4.6 Variation of radiation patterns with slot width at 2.45 GHz and 5.5 GHz.....	44
Figure 4.7 Slot-loaded rectangular patch	45
Figure 4.8 The dual slot architecture.....	46
Figure 4.9 Variation of reflection coefficients with slot radius R_1	46
Figure 4.10 Variation of radiation patterns with slot radius R_1 at 5.5 GHz.....	47
Figure 4.11 Variation of reflection coefficients with slot arc angle α	47
Figure 4.12 Variation of radiation patterns with slot arc angle α at 5.5 GHz	48
Figure 4.13 Variation of reflection coefficients with slot width	49
Figure 4.14 Variation of radiation patterns with slot width at 5.5 GHz.....	49
Figure 4.15 Optimum return loss.....	50
Figure 4.16 Surface current of disc.....	50
Figure 4.17 3D radiation patterns of the dual slot discone antenna	51
Figure 4.18 The quad slot architecture	52
Figure 4.19 Variation of reflection coefficients with slot radius R_1	53
Figure 4.20 Variation of radiation patterns with slot radius R_1 at 2.45 GHz and 5.5 GHz.....	53
Figure 4.21 Variation of reflection coefficients with slot arc angle α	54
Figure 4.22 Variation of radiation patterns with slot arc angle α at 2.45 GHz and 5.5 GHz	54
Figure 4.23 Variation of reflection coefficients with slot width W	55
Figure 4.24 Variation of radiation patterns with slot width W at 2.45 GHz and 5.5 GHz	55
Figure 4.25 S11 parameters of the final design	56
Figure 4.26 Radiation patterns of final design at 2.45GHz and 5.5 GHz.....	56
Figure 4.27 Total efficiency of the antenna	57
Figure 4.28 Surface current of disc.....	57
Figure 4.29 3D radiation patterns of the quad slot discone antenna.....	58

Figure 4.30 Final configuration of quad slot disccone antenna58

List of Tables

Table 1.1 Summary of IEEE 802.11 a/b/g/n Standards	2
Table 1.2 Requirements of antenna	3
Table 2.1 Summary of the different antennas characteristics	18
Table 3.1 Parameters of proposed antenna.....	22
Table 3.2 Cutoff frequencies for the first few values of m and n [32].....	25
Table 3.3 Values of P'_{nm} for TE modes of a circular waveguide [32]	26
Table 3.4 Values of P_{nm} for TE modes of a circular waveguide [32]	27
Table 3.5 Field lines for the TEM and TE_{11} modes of a coaxial line	29
Table 3.6 Optimized parameters	36
Table 4.1 Parameters of final design	59
Table. A Processing conditions of Preperm® L440	62
Table. B Characteristics of Preperm® L440.....	63
Table. C Characteristics of RG402/U.....	64

1 Introduction

1.1 Background of the Research

With the development of wireless communication, Wireless Local Area Networks (WLAN) are supporting and replacing wire networks at home and public. As the essential part of wireless communication systems, antennas enable high speed transmission of information and stable signal of the telecommunication. The increasing number of users in the primary unlicensed frequency bands 2.4 GHz and 5.5 GHz urge the antenna engineers to develop antennas with performance sufficient to support emerging applications. Challenging research subjects such as bandwidth enhancement, omnidirectional radiation patterns and antenna miniaturisation techniques are getting more and more popular.

1.2 Objectives

The objective of this master thesis is to design a transmitting antenna that suits the applications of access point working under the IEEE 802.11 a/b/g/n protocol. Several antennas that are suitable for these protocols have been proposed in literature, nevertheless, the design and implementation of the antenna presents many challenges.

The major 802.11 Wireless Local Area Network (WLAN) standards are summarized to provide users with a clear view of the specifications of the protocol. The latest IEEE Std 802.11 [1] shows the WLAN Medium Access Control (MAC) and Physical Layer (PHY) specifications. In Table 1.1 a generalization of the frequency ranges of IEEE Std 802.11a/b/g/n is presented [2][3].

Table 1.1 Summary of IEEE 802.11 a/b/g/n Standards

	802.11a	802.11b	802.11g	802.11n
Date of standard release	Sep 1999	Sep 1999	June 2003	Oct 2009
Bandwidths (MHz)	675	83.5	83.5	83.5, 675
Frequency range (GHz)	5.15-5.825	2.4-2.4835	2.4-2.4835	2.4-2.4835, 5.15-5.825
Max Data Rate (Mbps)	54	11	54	150
Channel width (MHz)	20	22	22	20 or 40
Range (m)	27-30	75-100	30	12-70

We find that the majority of access points in the market are using dipole antennas as transmitter antennas. However, from the industrial design point of view, an internal antenna is more popular than an external antenna for end users, thus, an antenna with compact dimensions is desired.

The radiating properties are one of the most important issues that need to be taken into consideration when designing an antenna. For most WLAN applications, the antennas are usually set on a table, on a ceiling, or mounted on the wall. For on-table antenna, it is required that the radiation pattern should be omnidirectional in the horizontal plane. For ceiling-mounted antennas, it needs to have a conical radiation pattern in the elevation plane. For wall-mount antenna, a broadside radiation pattern is preferred. The detailed requirements of the antenna are given in Table 1.2.

Table 1.2 Requirements of antenna

Parameters	Requirements
Frequency range (GHz)	2.4-2.4835, 5.15-5.825
Percentage Bandwidth	≥4.08% at lower band, ≥12.7% at higher band
Directivity	≥+3 dBi (2.45 GHz, 5.5 GHz)
Radiation patterns	Omnidirectional (azimuth plane), Conical (elevation plane)
Efficiency	≥85%
Feeding	SMA connector via semi-rigid cable
Dimensions	a×b×c, max (a, b, c) < 4 cm
Distance from antenna to users	≤10 m

1.3 Challenges

So far, there are plenty of published designs of WLAN antennas working under the protocol of IEEE 802.11 with impressive performance. Nevertheless, in current state of the art, none of these antennas can satisfy all our requirements. To let the antenna meet all requirements, remains a daunting task for us.

- Our primary challenge is to achieve the required operational bandwidth. The percentage bandwidth BW_p is defined by the formula [4]:

$$BW_p \triangleq 100\% \times \frac{BW}{f_c} \quad (1-1)$$

where f_H , f_L are the maximum and minimum frequency at -10 dB, respectively,

BW is the nominal bandwidth defined by $BW = f_H - f_L$,

f_c is the central frequency which defined by $f_c = (f_H + f_L)/2$.

The percentage bandwidth of this proposed antenna should be at least 4.08% at 2.45 GHz and 12.7% at 5.5 GHz. It is a challenge to let the antenna resonate at these two fixed frequencies. If the antenna system fails to cover all channels of IEEE 802.11 a/b/g/n protocol, it will not be able to guarantee the best communication quality.

- This project requires the antenna's radiation pattern to be omnidirectional at resonant frequencies. The most difficult challenge for us is to achieve similar antenna radiating properties for both bands. Usually, this is a daunting task because it has been found that multi-band antennas' radiating properties are quite variable at different frequencies. For typical disc antenna, the radiation pattern peaks usually move towards the cone as the frequency increases [5]. Good communication quality can be achieved if the antenna patterns on both frequencies are similar.
- Because the manufacturing technology of electronic device tends miniaturized, it is necessary to reduce the size of the antenna in design. However, a reduction in antenna size often results in a bandwidth reduction, lower gain, lower efficiency or worse impedance matching. Thus, the miniaturization techniques proves to be another challenge. Sometimes, performance has to be sacrificed a little in order to meet the basic demands of the system. In this thesis, the introduction of a dielectric material is used to reduce the dimensions of the antenna.

1.4 Approaches

In this project, we used several approaches to overcome the challenges and achieve the requirements.

- A literature study related to the state-of-the-art in dual-band WLAN antennas reveals that the disc antenna has outstanding bandwidth performance and better radiation pattern than other types of antennas. So this antenna type has been selected as the basis for new antenna development.
- To miniaturize the antenna the disc antenna was filled with dielectric material. This method not only largely reduces the antenna size, but also mechanically stabilizes the antenna.
- Thirdly, in order to achieve better performance of antenna radiation patterns, the effect of different types of slot on the disc were studied, and the novel quad-sector slot was suggested to be on the disc to maintain the similar radiation patterns on 2.4 GHz and 5.5 GHz frequencies.

1.5 Novelties

- This antenna has very compact dimensions, with a volume of 20 mm×20 mm×18.5 mm, which is much smaller than the conventional WLAN antennas.
- The frequency range of this antenna covers the bandwidth from 2.25 GHz to 6.0 GHz; it covers the frequency ranges of the major 802.11WLAN standards (2.4-2.4835, 5.15-5.825). This antenna can be used for dual band applications with only one element instead of multiple elements.
- The wideband operation of this antenna not only satisfies the requirements as a WLAN transmitting antenna, but also has great potential for other wideband applications.
- This antenna has an omnidirectional pattern in the horizontal plane and has a conical radiation pattern in the elevation plane. Such radiation properties are quite desirable for WLAN applications.
- The radiation patterns are similar conical patterns at both working frequencies, for most multi-band and wideband antennas, the radiation patterns are quite variable in terms of operating frequencies.
- The directivity of this antenna is 3.07 dBi at 2.45 GHz and 5.3 dBi at 5.5 GHz. compare with typical dipole antennas which directivities are always within 2.15 dBi [21], this proposed antenna has outstanding performance for WLAN utilizations.
- A novel slot cave on the disc of the antenna was also presented, the change of the slot width and length was used to adjust the radiation pattern direction and the input impedance of the antenna.

1.6 Thesis Outline

This thesis is organized in 5 chapters as follows:

Chapter 2: The state of the art in WLAN antennas are demonstrated in this chapter, 6 types of candidate antennas were analysed and compared, based on its comparative advantages with other antennas, finally the discone antenna was chosen.

Chapter 3: The discussions of numerical results are demonstrated in this chapter. The analysis of different antenna configuration is thoroughly investigated. Simulation results of the optimum dielectric covered discone antenna are illustrated in section 3.3.

Chapter 4: Based on the study of chapter 3, the novelties of discone antenna are shown in the beginning of this chapter, 3 types of slots were proposed and the optimal slot architecture was chosen to achieve better result.

Chapter 5: The conclusion of this report and future work suggestions and recommendations are given in this chapter.

2 State of The Art in WLAN Antennas

2.1 Introduction

The requirements for this thesis project was discussed in the first chapter, we need to design an omnidirectional antenna with a resonant frequency that covers the 2.4-2.4835 GHz and 5.15-5.825 GHz bandwidths. Several types of antennas are considered for this project. In this chapter a comparative study of these antennas is presented.

2.2 MIMO Antenna Systems

Multiple-input and multiple-output (MIMO) antenna systems are a common choice for wireless communication systems. Beam scanning or reconfigurable antennas for WLAN applications are designed because they can increase the capacity of the system without using extra spectrum and show a good reliability for communication systems.

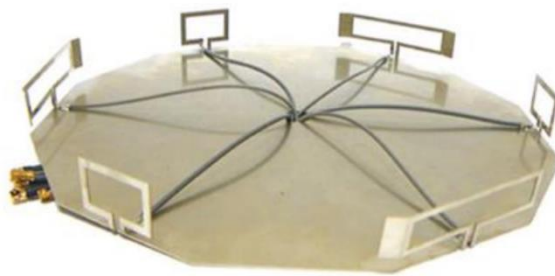


Figure 2.1 Configuration of the six-loop-antenna MIMO system [6]

In [6], a six-loop-antenna MIMO system operation in WLAN/WiMAX is reported (Figure 2.1). The loops are located on the edge of a ground plane to achieve evenly distribute radiation patterns. Similar MIMO antenna systems can be found in [7] and [8], in which the loop elements are replaced by monopoles located on the edge of the ground plane. This six-loop-antenna MIMO system is particularly designed for router and access point applications. This proposed MIMO sys-

tem met the requirements for majority WLAN applications. By adding the ground plane, this antenna has sufficient radiation gain. Furthermore, the radiation patterns are conical in the elevation plane at 2.4 GHz and 5.5 GHz. It enables better signal coverage when the antenna is mounted at the ceiling.

An obvious disadvantage of this antenna system is its large dimensions, even though it is a low-profile antenna, the antenna elements are located at the edge instead of at the centre of the ground plane. This creates difficulties for system implementations. Another drawback of the MIMO system is the complexity of differential feeding and mutual coupling between elements.

2.3 Planar Inverted F-Antennas (PIFA)

Planar Inverted F-Antennas (PIFA) are widely chosen for WLAN applications. Antennas of this type are particularly suitable for mobile terminals since they are compact, low profile and ease of fabrication. The PIFA typically consists of a planar element located above a ground plane, a shorting pin, and a feeding mechanism for the planar element [9], see Figure 2.2.

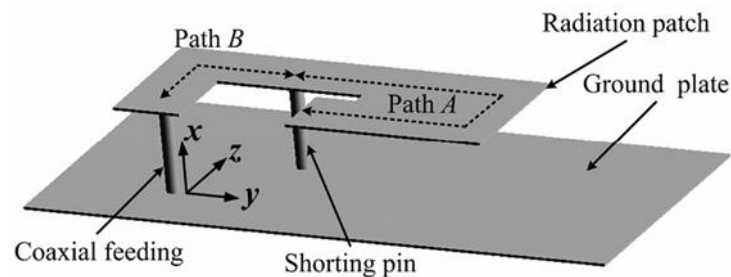


Figure 2.2 Geometries of PIFA antenna [9]

The antenna can achieve a multiband operation through the slot-loading technique on the planar element. In [10] the PIFA achieved quad-band operation by making three U-shape slot on the planar element. [11] studied the ground plane effects on the PIFA antenna. It is found that the bandwidth of PIFAs usually depends on the ground plane's dimensions. To achieve sufficient bandwidth for wireless communication, the length of the ground plane needs to be at least 0.8λ , which can be up to 100 mm at 2.4 GHz. Although a modified ground plane can make the antenna ultra-thin [12], it is difficult to reduce the dimensions of ground plane without sacrificing antenna

performance. The size of the PIFA's ground plane does not only significantly influence the antenna radiation pattern, but it also introduces high cross polarization in the horizontal plane when the dimensions of the ground plane are small.

An obvious drawback that we cannot compromise is PIFA antenna's poor radiation pattern. In [13], the antenna's radiation pattern is similar to omnidirectional at lower frequency, but the antenna pattern becomes unacceptable for higher frequency. As a receiving antenna, the antenna pattern do not need to be perfect, however, our task is to design an omnidirectional radiation pattern transmitting antenna. The PIFA's antenna patterns are not sufficient for our requirements.

2.4 Dielectric Resonator Antennas

Dielectric resonator antennas have been used in microwave circuits as oscillators and filters for a long time and it started to be used as radiators in recent decades. Figure 2.3 shows 3 typical dielectric resonator antennas (Rectangular DRA, Cylindrical DRA, and Hemi-spherical DRA) and their feeding methods. The dielectric resonator antenna has obvious advantages over other antennas: broadband operation, high efficiency, simple geometry, compact dimensions, single feed, and moderate beam width [14].

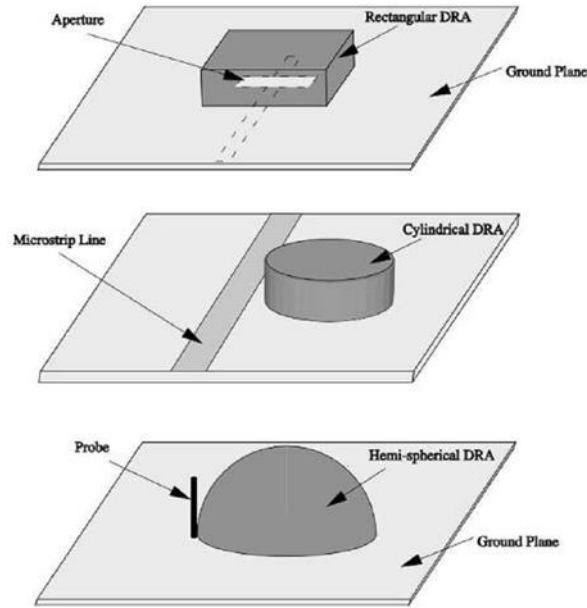


Figure 2.3 Typical dielectric resonator antenna and feeding mechanisms [14]

When designing a dielectric resonator antenna, material with lower permittivity is desired because lower Q-factor is necessary to improve the impedance bandwidth. The antenna dimensions can be reduced with high permittivity material, since [14]

$$\lambda \propto \frac{1}{\sqrt{\epsilon}}, \quad (2-1)$$

It is a challenge to design the compact size dielectric resonator antenna for lower frequency band applications.

DRA has the wideband operation which can be obtained through two methods: by lowering the inherent Q-factor of the resonator or using external matching networks and combining multiple resonators with different working frequency. However, these two methods mentioned above not only increase the complexity of the system but also raise the manufacturing cost largely. Consequently, it is more desired to integrate several modules of different frequencies into one piece. In [15], a hybrid dielectric resonator antenna suitable for dual-band WLAN application is presented. In this design, the combination of a monopole and a rectangular dielectric resonator reduces the antenna dimensions effectively. In [16], a similar design is reported. The common parts in the two designs are that the antenna dimensions are reduced largely by adding dielectric material.

Radiation pattern of the antenna are also what we care about. In [17] we can observe that the radiation patterns largely depend on the antenna shape.

2.5 Dipole Antennas

Dipole antennas are the most basic configurations and they are versatile for many applications. Dipoles are widely chosen by engineers because of their simple geometry, which can keep the computation to the minimum when designing. Dipole antennas are considered as a candidate antenna for our project because they can be used to achieve dual-band. Moreover, dipole antennas have omnidirectional radiation patterns in the azimuth plane instead of directional radiation patterns, which is essential for WLAN applications.

Apart from conventional geometries, many modifications have been done to make dipoles suitable for WLAN applications. For the dual-band WLAN dipole antenna in [18], the width of the printed dipole is widened to change the input impedance values at its higher frequency. It is also found the 5 GHz operational frequency can be shifted by cutting 45° chamfering at the feeding. Studies show that multi-band antennas can be obtained through the combination of several dipoles, authors in paper [19] presents a printed antenna which is comprised of three pairs of dipoles placed back to back to make them operate at triple-band of 2.4 GHz, 5.2 GHz and 5.8 GHz.

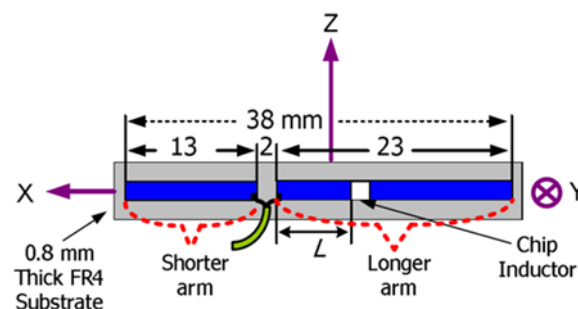


Figure 2.4 Geometry and detailed dimensions of a 2.4/5.2 GHz dual-WLAN unequal-arms dipole antenna [20]

In [20], a dual-band unequal-arms dipole antenna printed on the FR4 substrate is demonstrated (shown in Figure 2.4). The advantage of this antenna is it has compact dimensions and light weight. A novel technique of this antenna is a chip inductor was applied on the longer arm to

block the inverted current from occurring; the operational frequency of the higher band (5.2 GHz) can be shifted by changing the position of the inductor.

Those dipole antennas mentioned above all have very compact dimensions, which are desired for modern WLAN system. However, we are looking for an antenna which has conical radiation pattern on the elevation plane, the basic dipoles only have omnidirectional radiation pattern on azimuth plane, which is not suitable for access points which placed on the ceiling. The bandwidth and radiation gain of such dipole antenna is just passable for the requirements in Table 1.2. Moreover, the antenna directivity of typical dipoles at lower frequency is always lower than 2.15 dBi [21], as a consequence, we cannot use dipole for our project.

2.6 Bow-tie Antennas

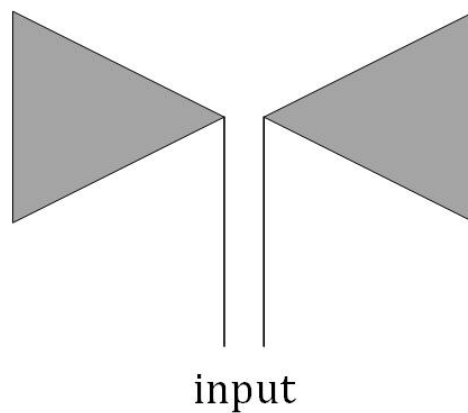


Figure 2.5 The bow-tie antenna

Broadband antennas have been used for WLAN applications through years. A wideband antenna can covers the main protocols of IEEE 802.11 without introducing extra antennas into the system. Typical wideband antennas like helical antennas, spiral antennas and bow-tie antennas have been investigated by researchers and have made remarkable results. Bow-tie antennas are widely chosen for wideband applications due to its simple geometry and ease of fabrication, see in

Figure 2.5. Such antennas are planer form of dipoles, whose radiation pattern is omnidirectional. Nevertheless, bow-tie antennas' typical gain are higher than conventional dipoles, about 5-6 dBi. However, the drawbacks of bow-tie antennas like limitation of the bandwidths cannot be neglect, the variation of it resistance and reactance are quite severe as a function of frequency. Consequently, over the years many methods are applied in order to increase its bandwidths. [22] and [23] investigate bow-tie antenna in wideband wireless communication system. For both cases the antennas cover the operational bandwidth of all the protocol of IEEE 802.11 Wireless Local Area Network (WLAN) standard. Cavities were added to the back of antennas not only to increase the gain but also to produce unidirectional patterns. However, such cavities largely increased the antenna volume, and did not make radiation patterns better.

2.7 Conical Antennas

In this section we discuss two types of conical antenna: biconical antenna and discone antenna. These two types of antennas' architectures are based on conical architecture. Since the radiating elements are volumes, the impedance bandwidths of such antennas are much wider than planar antennas.

2.7.1 Biconical Antennas

Biconical antennas (see Figure 2.6) can be considered as three-dimensional form of the bow-tie antennas. Part of the energy along the antenna surface is reflected and most of the energy is radiated near the equator, consequently, cone antennas have the omnidirectional radiation patterns on azimuth plane. Moreover, they have better bandwidths potential compare to bow-tie antennas because the variations of their resistance and reactance are less severe as a function of frequency. The common model of biconical antenna is shown in Figure 2.6.

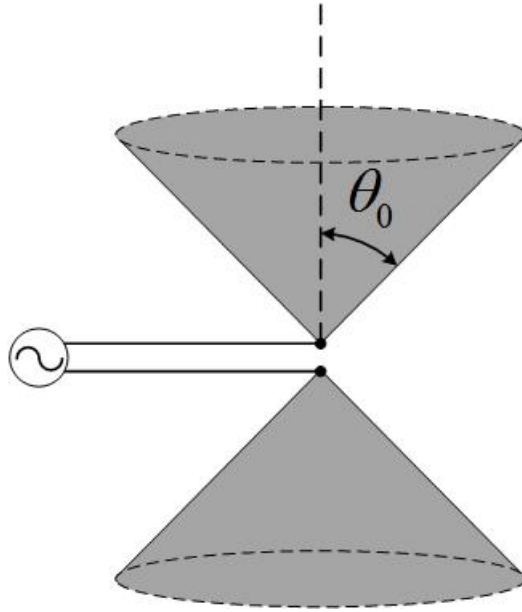


Figure 2.6 The biconical antenna

For infinites cones, the input impedance are modelled by [24]:

$$Z_{in} = 120 \ln(\cot(\frac{\theta_0}{2})), \quad (2-2)$$

where θ_0 is the half-cone angle.

From equation (2-2) we can find for the transmission line with input impedance 50Ω , the half-cone angle could be very wide. We can find the antenna's bandwidth increases with the cone angle [25]. Although it is not very critical in antenna design, very small or very wide angles are not so practical in designs.

The conical antennas are transformation of biconical antennas by changing the upper cone into an infinite plane. It has been earlier analysed by Smith P.D.P in 1948 [26], Papas and King in 1949 [27]. It has a good potential for WLAN applications due to its wideband operation and omnidirectional radiation pattern in the horizontal direction.

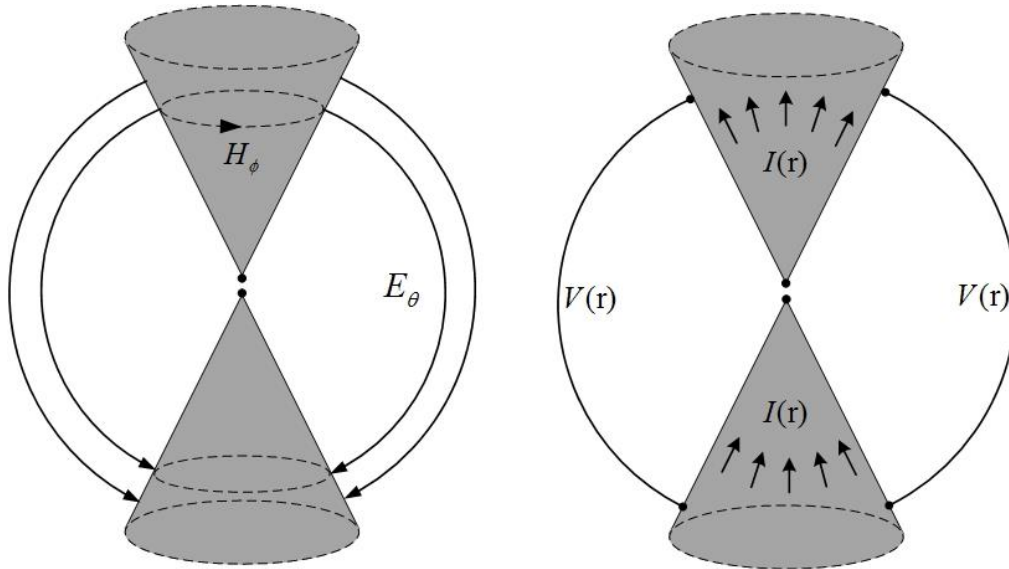


Figure 2.7 Electric and magnetic fields, and associated voltages and currents, for a biconical antenna

The voltage at the input terminals produces the electric and magnetic fields around the biconical antenna. The current distribution on the biconical surface is showed in Figure 2.7.

The field distribution of biconical antenna is symmetrical, and the radiation pattern on the azimuth-plane is omnidirectional.

One obvious drawbacks of the conical antenna is the large dimensions and three-dimensional structure, which bring difficulty for fabrication or implementation in limited space. However, many studies have been done to reduce its dimensions and complexity of the architecture. In [28] the dielectric material was added outside the conical structure to reduce the dimensions and stabilize the conical. The antenna configuration is shown in Figure 2.8.

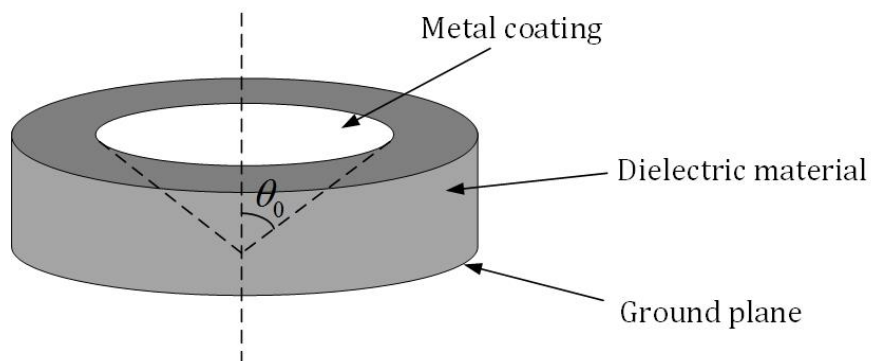


Figure 2.8 Dielectric covered conical antenna

The conical and the ground plane can be regarded as a piece of transmission line with characteristic impedance [29]:

$$Z_0 = \frac{1}{\pi} \sqrt{\frac{\mu_0}{\epsilon_r \epsilon_0} \ln(\cot(\frac{\theta_0}{2}))}, \quad (2-3)$$

where $\epsilon_0 = 8.854 \times 10^{-12} \text{ F/m}$ is the permittivity of free space,

$\mu_0 = 4\pi \times 10^{-7} \text{ H/m}$ is the permeability of free space,

ϵ_r is the relative permittivity of the dielectric material,

θ_0 is the half-cone angle.

The cone angle θ_0 is directly related to ϵ_r . In free space, when the antenna characteristic impedance equal to 50Ω , we can calculate the cone angle θ_0 :

$$\theta_0 = 80^\circ$$

The conical antenna with such wide angle will be difficult to fabric. However, when dielectric material is covered outside the conical antenna, for instance, $\epsilon_r = 4.4$, then we have the cone angle θ_0 :

$$\theta_0 = 50^\circ$$

In practice, the result can be deviated from the calculated result.

2.7.2 Discone Antennas

The discone antennas are another form of conical antenna, such antenna consists of a disc and a cone, feeding by a coax in the centre of the cone, where the outer shield of coax is connecting to the lower cone and the centre conduct is connect to the disc [30]. A discone antenna has similar characteristic of a biconical antenna but only half of its volume. By optimizing the dimensions of the disc and the cone we can obtain wide bandwidth.

The disc on the top is finite compare with infinite conical antenna. Similarly, such antenna has the advantages of simple mechanical design, ease of installation and broadband operation. Moreover, discone antennas have conical radiation patterns on the elevation plane.

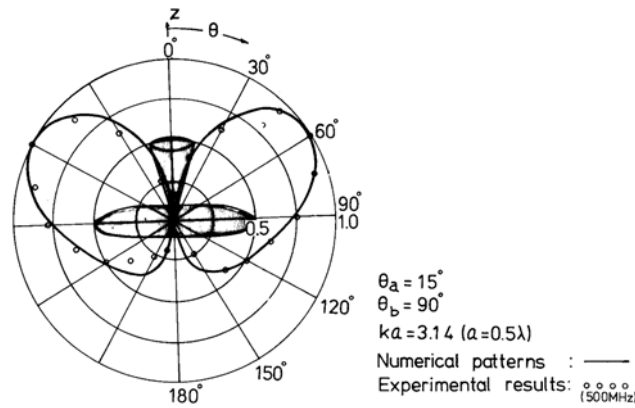


Figure 2.9 Normalized pattern of disc antenna [31]

Figure 2.9 shows a normalized pattern of disc antenna at 500MHz [31], the patterns of disc antenna are omnidirectional at azimuth plane and a conical pattern at the elevation plane. The radiation pattern peaks usually moves towards the cone as the frequency increases [5]. As mentioned in chapter one, the antenna of this project is particularly designed for the router and access point applications, so the conical radiation patterns in the elevation plane is particularly desired for better indoor signal coverage.

Similar to conical antennas, the operational wavelength of disc antennas are proportional to their dimensions. As a result, the disc antenna's volume could be massive for lower operational frequency. This phenomenon makes disc difficult to integrate into applications where space is extremely limited. Theoretically, the height of cone is $\lambda/3$ in free space [25], so the dimensions of disc are larger than 40 mm under 2.4 GHz frequencies. As mentioned in section 2.7.1, the miniaturization technique of the antenna can be realized by using the dielectric material.

There are also triangular-sheet and wire-simulation cone surface, such structures can reduce the weight and have less wind resistance. However, these structures have very narrow bandwidth compare with solid disc. Since this project is indoor application and have strict requirements for bandwidth, we should use solid disc in this project.

2.8 Conclusion

In this chapter we discussed six typical antennas which suitable for WLAN applications. These antennas are designed with compact dimensions and usually applied on the mobile terminal. Each antenna has its outstanding performance on one aspect or another. However, they also have a few drawbacks make them not sufficient for the requirements of our project. The six-loop MIMO antenna system has good bandwidth and sufficient realized gain, but the dimensions and the feeding complexity make it less attractive for the application, moreover, the radiation patterns of it is not precisely omnidirectional. PIFA antennas are outstanding in compact dimensions, low cost and simple geometry, but the radiation patterns are unacceptable as a transmitting antenna. Dielectric resonator antennas are good candidate antennas as a wideband antenna, but its massive volume and manufacture cost makes it not preferred candidate antenna. Dipole antenna has advantages of compact size, simple geometry and low cost, however its radiation patterns do not have a conical radiation pattern in the elevation plane, which makes it not good enough for WLAN transmitter antenna. Bow-tie antennas have good potential because of its simple geometry and easy for manufacture, however its limitation on bandwidth and less satisfying radiation patterns are the drawbacks we cannot neglect. Finally we discussed conical antennas and found discone antennas have best performance over other antennas for our project.

Table 2.1 provides a clear overview of the different antennas characteristics we discussed above.

Table 2.1 Summary of the different antennas characteristics

EM characteristics	MIMO antenna systems	DRAs	PIFAs	Dipole antennas	Bow-tie antennas	Conical antennas
Impedance BW	-	+	-	-	+	+++
Gain	+	++	-	+	++	+++

Dimensions/Weight	--	--	+	+++	+	-
Radiation patterns	+	--	---	-	++	+++
Manufacture cost	--	--	++	+++	+++	+
Architecture Simplicity	---	+	+	+++	+++	+

“+++” represents performance very desirable, “---” represents performance very undesirable.

Others are different degree in between.

3 Numerical Analysis of the Dielectric Filled Discone Antenna

3.1 Introduction

In Chapter 2 several types of WLAN antennas was discussed, and the discone antenna was considered to have advantages over other antenna configurations. In this chapter, we proposed a novel discone antenna which has wideband operation and omnidirectional radiation pattern. The inspiration for this antenna comes from [28]. In order to reduce the antenna dimensions, dielectric material was used to fill in between the discone antenna and the ground plane. The numerical analysis and optimization of antenna are also demonstrated in this chapter.

3.2 Overview of the Design

The antenna's architecture and side view are shown in Figure 3.1, the discone antenna was placed on a metallic ground plane, and the dielectric material was filled in between discone antenna and the ground plane which form a cavity. The antenna is fed through a 50Ω coax cable at the bottom. The detail explanation of parameters and optimization start value can be found in Table 3.1.

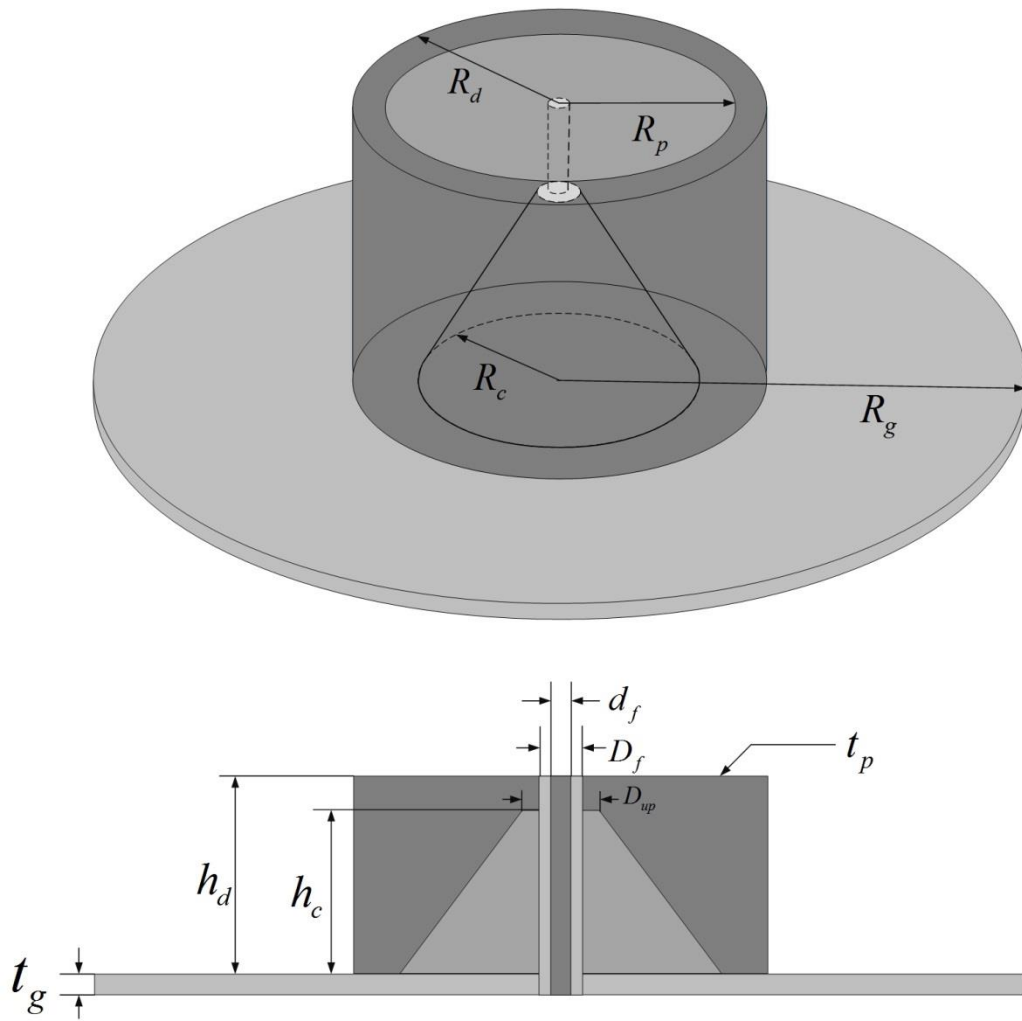


Figure 3.1 Disccone antenna filled with dielectric material

Table 3.1 Parameters of proposed antenna

Parameters	Descriptions	Optimization start value
R_d	Radius of dielectric material	20 mm (fixed)
h_d	Discone overall height	17.5 mm
t_p	Thickness of disc	0.035 mm (fixed)
R_p	Radius of disc	15 mm
D_{up}	Upper cone diameter	3.47 mm (fixed)
R_c	Radius of cone	20 mm
h_c	Height of cone	15 mm
R_g	Radius of ground plane	50 mm
t_g	Thickness of ground plane	1 mm (fixed)
D_f	Diameter of feeding coax line	2.97 mm (fixed)
d_f	Diameter of feeding coax pin	0.91 mm (fixed)

3.3 Optimization Procedure

The optimization procedure of proposed antenna was carried out in the following sections. The optimization parameters can be found in Table 3.1, parameters such as R_d , t_p , D_f , d_f are already fixed in the design and will not change in the optimization procedure, we will optimize the rest six parameters step by step to obtain the best performance in terms of the bandwidths and radiation patterns.

3.3.1 Analysis of Waveguide Cavity

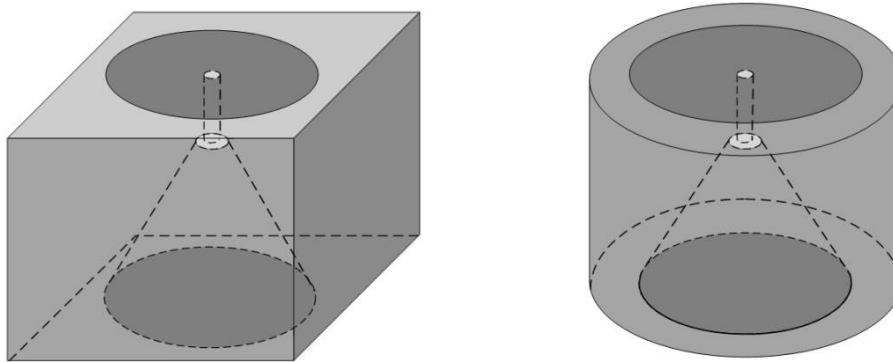


Figure 3.2 Proposed cavity models

Before we design the antenna, two types of cavity were considered for this project, the rectangular waveguide cavity resonators and circular waveguide cavity resonators. The configurations of two cavity models can be found in Figure 3.2. Although both cavity models can be applied for our project, we choose circular waveguide cavity resonators for our project. The detail analysis is demonstrated in the following part.

Rectangular Waveguide Cavity Resonators

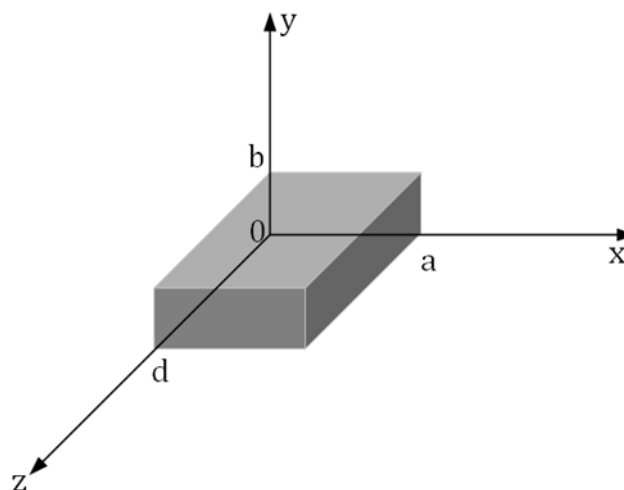


Figure 3.3 Rectangular Waveguide Cavity resonators

Cavity is formed through the short circuited at both ends of the microwave resonators, so as to reduce the magnificent radiation loss at the open end of the resonators. Figure 3.3 shows a rectangular cavity resonator. The electric and magnetic energy is stored inside the cavity and power is dissipated on the wall of cavity and the dielectric material filled in.

The resonator frequency of TE_{nm} or TM_{nm} mode in rectangular cavity is [32]:

$$f_{cnm} = \frac{c}{2\pi\sqrt{\epsilon_r}} \sqrt{\left(\frac{m\pi}{a}\right)^2 + \left(\frac{n\pi}{b}\right)^2} \quad (3-1)$$

Certain modes can be excited at a given frequency for a given cavity size. The cavity must be an integer multiple of a half-guide wavelength long at the resonant frequency.

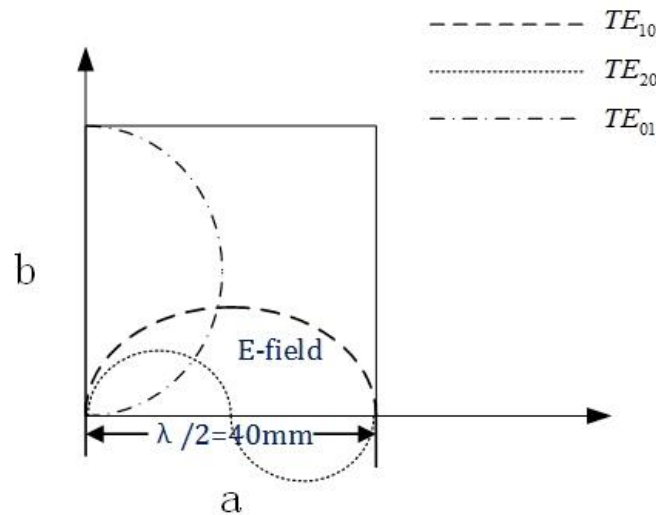


Figure 3.4 Cut plane of the square waveguide

Equation (3-1) shows the cutoff frequency of the cavity is inverse proportional to the dimensions, the dielectric resonator antennas' dimensions are in the order of $\lambda_0 / \sqrt{\epsilon_r}$, so the size of antenna could be very compact by using high permittivity material at high frequencies. The dual-band operation can be obtained through excitation of two resonant modes simultaneously.

Figure 3.4 shows the cut plane of the cavity, in this program, the maximum dimensions of cavity should be within $40\text{mm} \times 40\text{mm}$, to let the desired mode exist and propagated through the cavity, the edge length of the cavity must be larger than a half of the guided wavelengths at the corresponding mode.

When $a=b=40\text{mm}$, we could calculate the cutoff frequencies of lower mode for air-filled square cavity, the result is shown in Table 3.2.

Table 3.2 Cutoff frequencies for the first few values of m and n [32]

Mode	m	n	f_c (GHz)
TE_{10}	1	0	3.75
TE_{20}	2	0	7.5
TE_{01}	0	1	3.75
TE_{11}, TM_{11}	1	1	5.3

We can find for the $40\text{mm}\times 40\text{mm}$ air-filled square cavity the lowest cutoff frequency is 3.75 GHz, which is much higher than first resonant frequency 2.4 GHz. Nevertheless there are two methods to decrease the cutoff frequency: one way is to increase the cavity dimensions. According to equation (3-1), if the cavity dimensions is $63\text{mm}\times 63\text{mm}$ works in TE_{01} mode, the cutoff frequency will be reduced to lower than 2.4 GHz. However, such large cavity dimensions fails to meet the requirements of our project, so it is not wise to use this method. Another method is to change the fill-in material of cavity, from equation (3-1), if we fill the square cavity with dielectric material instead of air, the cutoff frequency will decrease as the permittivity ϵ_r increases. By choosing the dielectric permittivity carefully, it is possible to reach the proposed cutoff frequency without increase the cavity dimensions. We should guarantee the cavity working bandwidth covers the required bandwidth (2.4 -2.484 GHz, 5.15-5.825 GHz).

Since higher mode will cause worse cross-polarization, if we only let TE_{01}, TE_{10} mode pass through the waveguide, the proposed cutoff frequency should be 2.4 GHz, take this value into equation (3-2) [32]:

$$\epsilon_r = \left(\frac{c}{f_c a} \right)^2 = \left(\frac{3 \times 10^8}{2.4 \times 10^9 \times 0.04} \right)^2 = 9.766 \quad (3-2)$$

We can derive the permittivity of the dielectric material $\epsilon_r = 9.766$.

Circular Waveguide Cavity Resonators

A cylindrical cavity resonator can be constructed from a section of circular waveguide shorted at both ends, see Figure 3.5.

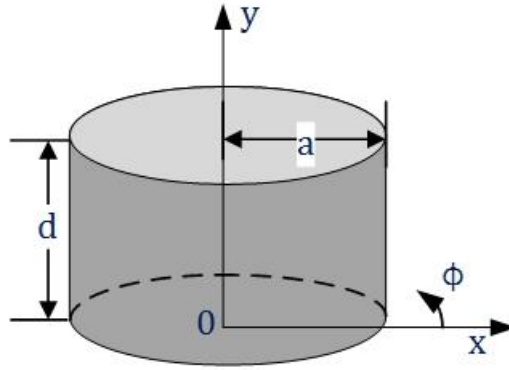


Figure 3.5 A cylindrical resonant cavity

The dominant cylindrical cavity mode is the TE_{11} mode and TM_{01} mode.

The cutoff frequency for the TE_{nm} mode is [32]:

$$f_{nm} = \frac{p'_{nm} c}{2\pi a \sqrt{\mu_r \epsilon_r}} \quad (3-3)$$

The cutoff frequency for the TM_{nm} mode is [32]:

$$f_{nm} = \frac{P_{nm} c}{2\pi a \sqrt{\mu_r \epsilon_r}} \quad (3-4)$$

P'_{nm} is the m th roots of J_n , where J_n is the Bessel functions of first kind.

Table 3.3 Values of P'_{nm} for TE modes of a circular waveguide [32]

First order of the Bessel function n	P'_{n1}	P'_{n2}	P'_{n3}
0	3.832	7.016	10.174
1	1.841	5.331	8.536
2	3.054	6.706	9.970

Table 3.4 Values of P_{nm} for TE modes of a circular waveguide [32]

First order of the Bessel function n	P_{n1}	P_{n2}	P_{n3}
0	2.405	5.52	8.65
1	3.83	7.06	10.17
2	5.13	8.41	11.62

The values of P'_{nm} and P_{nm} for TE modes of a circular waveguide are shown in Table 3.3 and Table 3.4, respectively. In this program, the low modes are preferred, because higher order mode will have worse cross-polarization of the antenna. However, we need to make the cutoff frequency to be as low as possible, so we take the Eigen value of TE_{11} mode, suggest $P'_{11} = 1.841$, we can calculate the permittivity of the dielectric material [32]:

$$\epsilon_r = \left(\frac{c \cdot P'_{nm}}{2\pi a f_c} \right)^2 = \left(\frac{3 \times 10^8 \times 1.841}{2\pi \times 0.02 \times 2.4 \times 10^9} \right)^2 = 3.35 \quad (3-5)$$

The calculated permittivity of the dielectric material is 3.35.

According to the analysis above, we can find when the cutoff frequencies and dimensions of the cavities are fixed, the filled in dielectric material of rectangular cavity always have higher permittivity. Since lower dielectric permittivity is desired in antenna design, we should choose circular cavity model for this project.

3.3.2 Choice of Dielectric Material

In previous section, we choose circular cavity model because the filled in material would have lower permittivity. Theoretically, if we do not need to take design volume in to account, it would be a good choice to use air as substrate material, in this condition, highest efficiency and maximum gain of the antenna will be obtained, and the impedance bandwidth will also be maximized and surface wave losses will be minimized. Yet the limitation of design space left for antennas force engineers to find a balance between performance and dimensions of the antenna.

In our project, the space left for antenna is limited, so the disccone antenna without dielectric material can be so massive and not suitable for some applications. In practical applications, the loss of the material always exists. Moreover, it increases with frequency. We would discuss the effect dielectric material bring for antenna design in the following part.

For dielectric resonator antennas, the bandwidth is in the order of Q-factor [25],

$$BW = \frac{s-1}{Q\sqrt{s}} \cdot 100\% \quad (3-6)$$

Where,

s is the desired VSWR at the input port of the DRA.

By decreasing the dielectric constant we can obtain lower Q factor, yet in this case, the size of the antenna will also increase.

In section 3.3.1 we can find when the dimensions and cutoff frequency of circular cavity is fixed, the dielectric permittivity $\epsilon_r = 3.35$, in practical design, we should let the dielectric permittivity higher than this value so that the cutoff frequency of circular cavity will be lower than 2.4 GHz. We find a low loss dielectric material Preperm® L440 which is suitable for our project. The dielectric permittivity of this material $\epsilon_r = 4.4$, and the loss $\tan \delta = 0.0005$ (Details of this material can be found in Appendix A).

3.3.3 Choice of Feeding method

Feeding Mechanism

As shown in Figure 3.1, the disccone antenna is feeding through a coaxial probe. The inner conductor of the coax is connected to the disc, and the outer conductor is connected to the cone. The configuration of coax cable is shown in Figure 3.6.

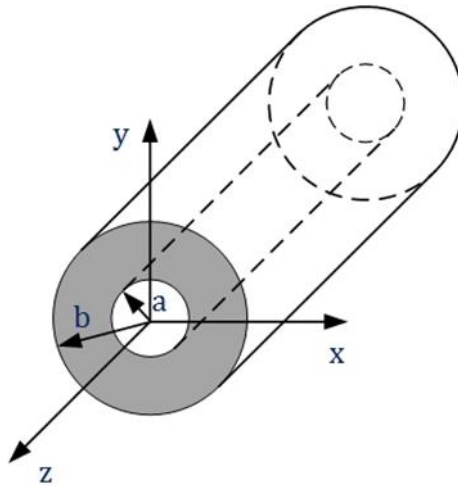


Figure 3.6 The coaxial cable

The coaxial feeding has many advantages over other feeding method. It is easy to fabric and has low spurious radiation. The coaxial line can supported transverse electric (TE) modes; transverse magnetic (TM) modes in addition to transverse electromagnetic (TEM) mode. The cutoff frequency of the coaxial cable is inverse proportional to its dimensions. Undesirable effects can occur if more than two modes propagating at the same time. So the propagation of higher order modes should be avoided.

Table 3.5 Field lines for the TEM and TE₁₁ modes of a coaxial line

TEM mode	TE ₁₁ mode

In coaxial cable, the dominant mode is the TEM mode, and the cutoff frequency of the coaxial cable for TEM mode:

$$f_c = 0$$

The cutoff frequency of the coaxial cable for TE_{11} mode [32]:

$$f_c = \frac{c}{(a+b)\pi\sqrt{\epsilon_r}} \quad (3-7)$$

Where a is the inner conductor radius of the coax cable.

b is the dielectric radius of coax cable,

c is the speed of light in free space,

ϵ_r is the relative permittivity of the dielectric material.

The cutoff frequency of TE_{11} mode could be much higher than our required operational frequency, so we should only let TEM mode through the coaxial line.

The characteristic impedance of a coaxial cable is primarily determined by the ratio of inner and outer diameters [33]:

$$Z_0 = \frac{60}{\sqrt{\epsilon_r}} \ln \frac{b}{a} \quad (3-8)$$

In this thesis project, the proposed antenna is fed by a circular coaxial line which has $Z_0 = 50 \Omega$ impedance, which is the most common value in antenna design applications. According to the calculation, the dimensions of the coaxial cable should satisfied value of $b/a=3.34$. There are several coaxial cables could meet the demand, we choose the semi-rigid cable RG402/U for this project.



Figure 3.7 Semi-rigid cables

Semi-rigid cables are inexpensive to purchase when compared to many other coaxial cable alternatives. See (Figure 3.7). Such cable comes as close as possible to the ideal coaxial cable so we

used it in this proposed antenna, the outer shield of the cable is solid copper. This type of coax is outstanding in shielding compared to cables with a braided outer conductor, especially at higher frequencies. The major drawback of such cable is lack of flexibility, yet this characteristic is suitable for some certain cases which flexibility is not desired.

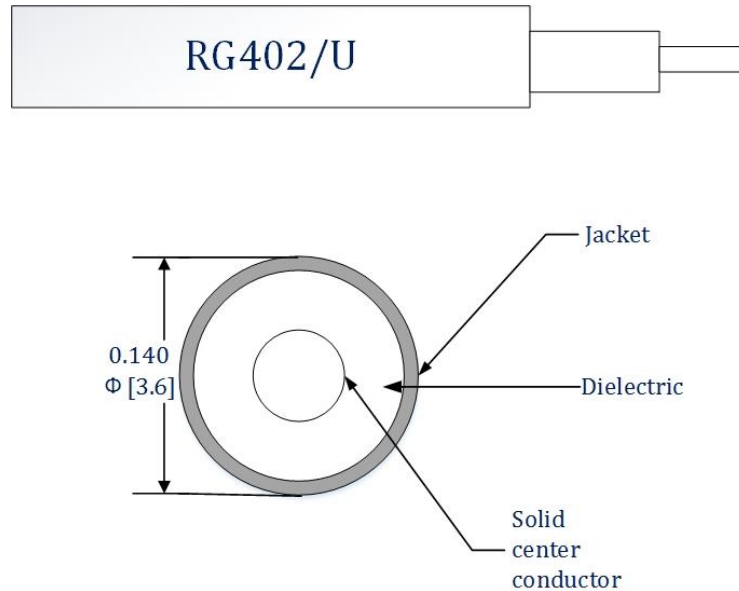


Figure 3.8 Geometry of the RG402/U coaxial cable

The coaxial feeding we used in this program is RG402/U [34], see Figure 3.8. The typical properties like physical and electrical specifications of RG402/U are showed in Appendix B. The dielectric material we use in the coaxial cable is Teflon, with the dielectric permittivity, $\epsilon_r = 1.99$. The electric loss $\tan \delta = 0.0004$.

3.3.4 Optimization of Cone

Optimization of Cone Height

As mentioned in section 2.7.2, the initial dimensions of the parameters are showed in Table 3.1. Our aim is to achieve the sufficient bandwidth which can cover the 2.4-2.4835 GHz, 5.15-5.825 GHz bandwidth. In free space, the height of cone is kept as $h_c = \frac{\lambda}{4}$ [35]. Since we filled the discone antenna with dielectric material, the theoretical cone height:

$$h_c = \frac{\lambda}{4\sqrt{\epsilon_r}} = 14.9\text{mm} \quad (3-9)$$

Hence, the optimization values for the cone height h_c we choose are:

$$h_c \in \{15, 16, 17\} \text{ mm}$$

Figure 3.9 shows the variation of s_{11} parameters in response to different cone heights. We can find when cone height is 16 mm the reflection coefficient is the deepest.

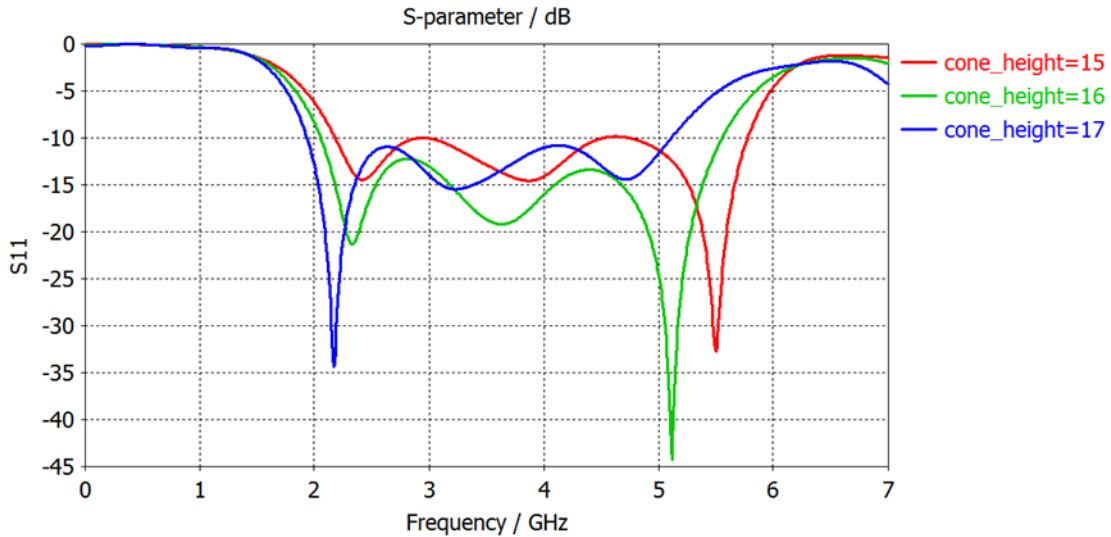


Figure 3.9 Optimization of the cone height

Optimization of Cone Radius

In section 2.7.1 we discuss the relation between half-cone angle and the dielectric permittivity. According to formula (2-3), we calculated the theoretical cone-half angle is 50° . Due to the limitation of the dimensions, the radius of cone is not more than 20mm.

The optimization values for the cone radius r_c we choose are:

$$r_c \in \{15, 16.5, 18\} \text{ mm}$$

Through the optimization in Figure 3.10, we found the antenna has best S_{11} performance when cone radius $r_c = 15$ mm. The upper radius of the cone is fixed value, we keep it as 3.47 mm, and the platform outside the coax cable is 0.25 mm wide.

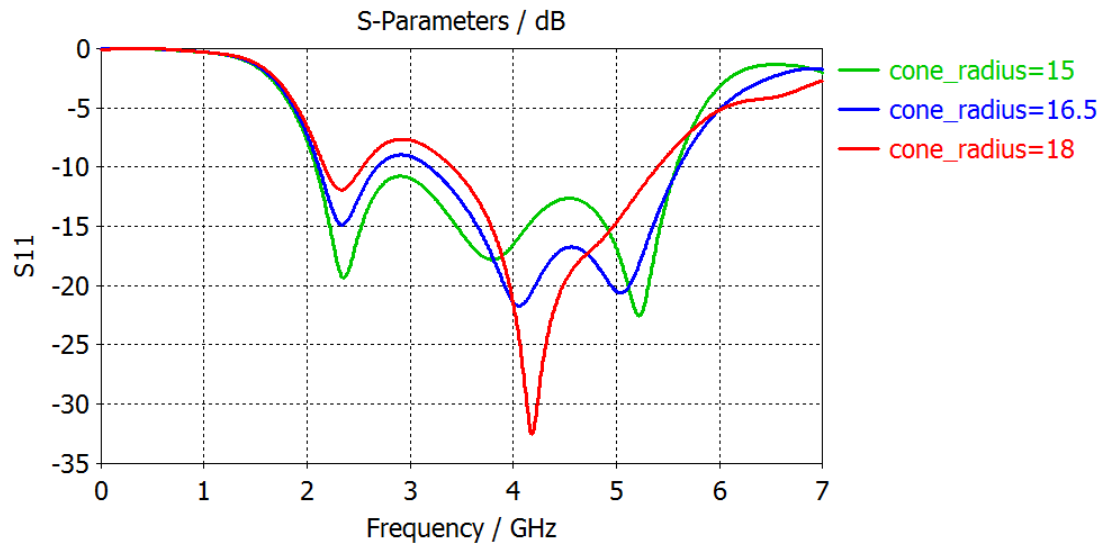


Figure 3.10 Optimization of the cone radius

3.3.5 Optimization of Disc

Optimization of Discone Height

Since the dimensions of the discone overall height is in terms of the wavelength,

The optimization values for the discone height h_d we choose are:

$$h_d \in \{17.5, 18.5, 19.5\} \text{ mm}$$

From Figure 3.11, we found when the overall height equals to 18.5 mm, the antenna has the best S11 performance.

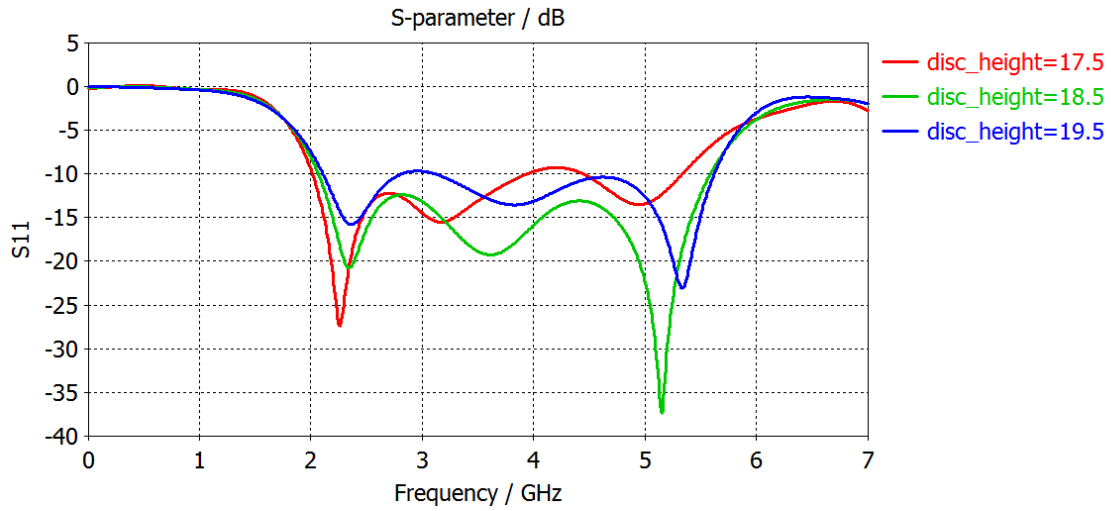


Figure 3.11 Optimization of discone overall height

Optimization of Disc Radius

The requirements of project limited the disc radius should be not more than 20 mm.

The optimization values for the disc radius r_p we choose are:

$$r_p \in \{17, 18, 20\} \text{ mm}$$

From Figure 3.12 we can find when the disc radius equals to 20 mm, antenna has the best impedance performance.

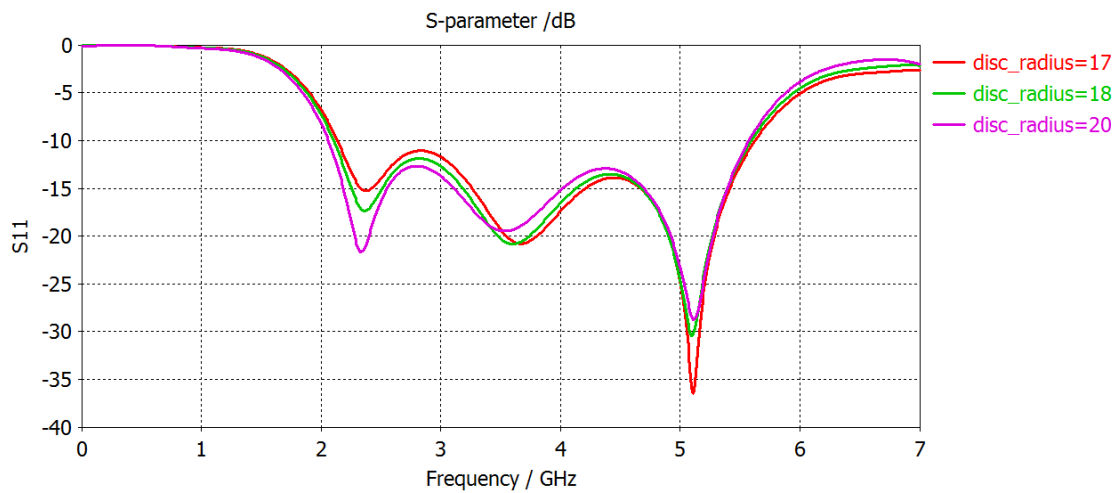


Figure 3.12 Optimization of disc radius

3.3.6 Optimization of Ground Plane Radius

The antenna gain and radiation patterns also depend on the size of ground plane. When the radius of ground plane is bigger, the antenna front-to-back ratio increases. The thickness of the ground plane does not influence the result much, so we keep $t_g = 1mm$, as it will not be too thick.

The optimization values for the discone height R_g we choose are:

$$R_g \in \{50, 60, 70\} \text{ mm}$$

Figure 3.13 shows the variation of reflection coefficient in terms of the ground plane radius, the antenna bandwidths do not vary much with different ground plane radius values, yet we can find that when ground plane radius $R_g = 60mm$, the reflection coefficient is deeper than the situation $R_g = 70mm$. Figure 3.14 shows the variation of polar radiation patterns in terms of the different ground plane radius, we can observe that the ground plane radius largely influence the antenna's radiation patterns, besides, the antenna's directivity is lower than 3 dBi when $R_g = 50mm$. It is essential to obtain best S11 parameters and radiation patterns at the same time. As a result, we chose $R_g = 60mm$.

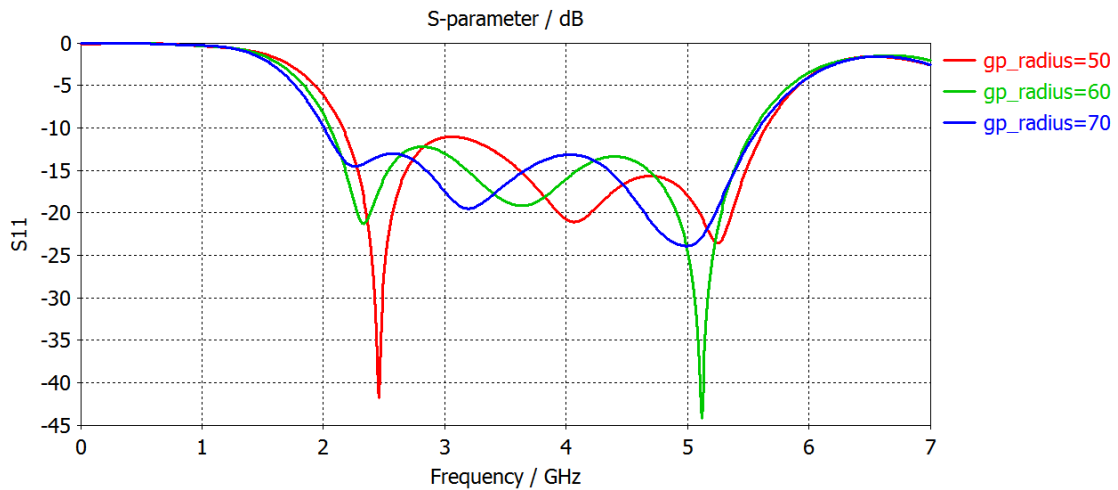


Figure 3.13 Optimization of ground plane radius

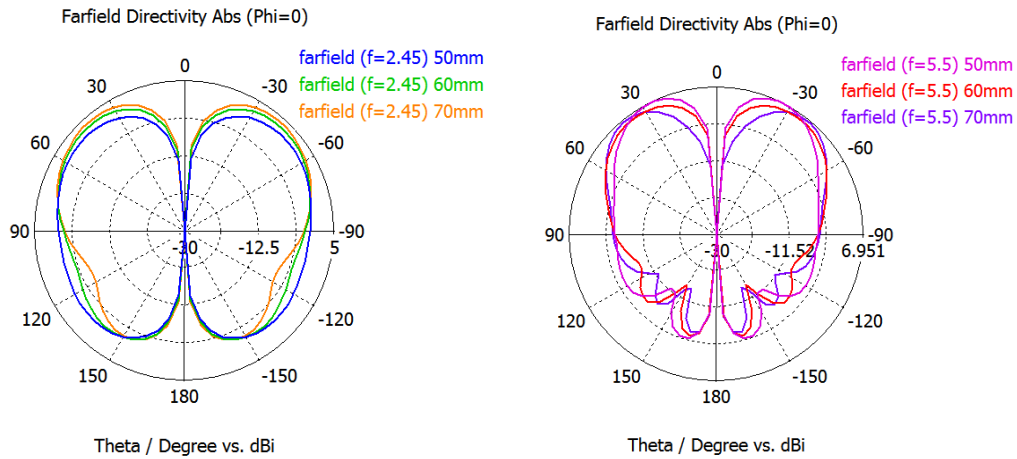


Figure 3.14 Variation of polar radiation patterns in terms of the different ground plane radius

3.4 Discussion of Antenna Performance

In the previous section we study the effect of parameter variation of antenna. The optimization value can be found in Table 3.6.

Table 3.6 Optimized parameters

Parameters	Descriptions	Optimization start value
R_d	Radius of dielectric material	20 mm (fixed)
h_d	Discone overall height	18.5 mm
t_p	Thickness of disc	0.035 mm (fixed)
R_p	Radius of disc	20 mm
D_{up}	Upper cone diameter	3.47 mm (fixed)
R_c	Radius of cone	15 mm
h_c	Height of cone	16 mm
R_g	Radius of ground plane	60 mm
t_g	Thickness of ground plane	1 mm (fixed)
D_f	Diameter of feeding coax line	2.97 mm (fixed)
d_f	Diameter of feeding coax pin	0.91 mm (fixed)

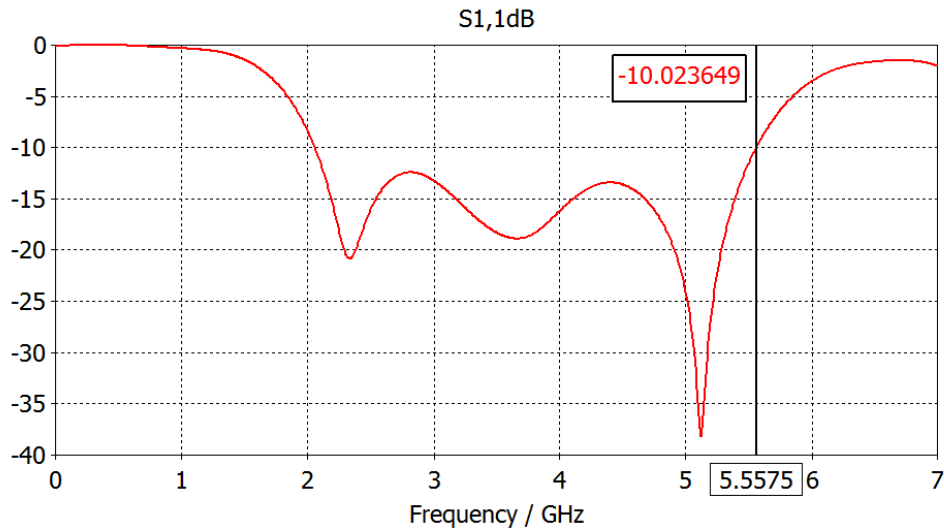


Figure 3.15 S11 parameters of the proposed antenna

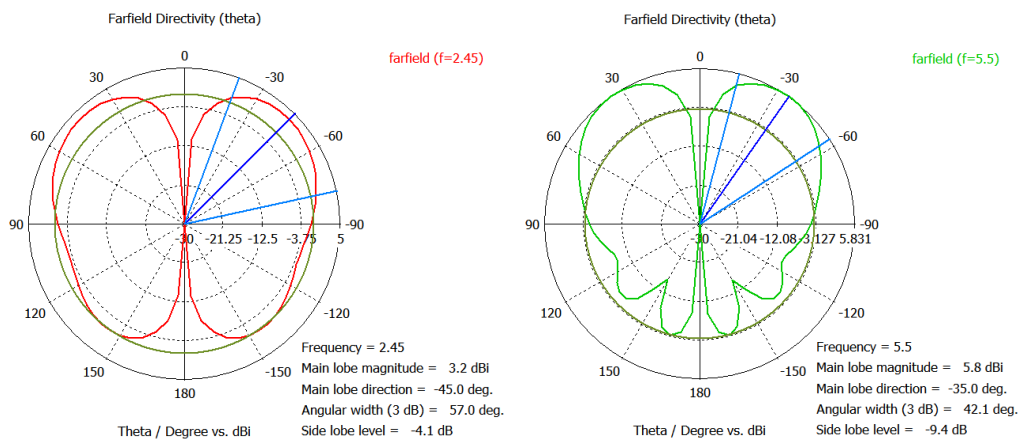


Figure 3.16 Polar radiation patterns of proposed antenna at 2.45 GHz and 5.5 GHz

The proposed antenna configuration is a combination of discone, cavity, dielectric material, ground plane. The operational bandwidth of antenna is 2.05-5.56 GHz (see Figure 3.15), it is sufficient to covers the lower resonant frequency (2.4-2.4835 GHz), but it does not fully cover the higher resonant frequency (5.15-5.825 GHz), we need to make improvement for its architecture in order to increase its bandwidth for higher frequency. The antenna directivity at both frequencies showed in Figure 3.16 are large enough to meet the +3dBi requirement of our project. What is less satisfactory is the main lobe width of 35° at 5.5 GHz which is much less compared with the 2.45 GHz radiation pattern. It is preferred to let the antenna achieve similar conical patterns at both frequencies.

It can be inferred from the result that this antenna did not provide the required bandwidth and radiation patterns, in order to make improvement on its performance; we proposed a novel slot cave on the antenna disc to achieve better impedance bandwidth and radiation patterns. This will be demonstrated in the next chapter.

4 Dielectric Filled Discone Antenna with Quad Slot

4.1 Introduction

It is known that the slots on the patch have the ability to obtain large bandwidths without adding parasitic elements. A variety of studies have shown that cutting slots of different shapes on the patch could improve the impedance matching of the patch antenna. This is because slots change the current paths on the radiators, separate the radiator into more than one resonant region for multi-band operation. The impedance matching is related to the size, location and shape of slots. The study in [36] illustrated the effects of the slots' shape, the large inductance caused by large space of slot can be compensated by increasing the slot length, and the capacitance of the antenna is influenced by width of the slot. Wider the slot, the larger capacitance will be.

In previous chapter, we have shown that the performance of dielectric filled discone antenna is not sufficient to meet the performance of our project. In order to achieve wider bandwidths and better radiation patterns, in this chapter we proposed 3 types of slots architecture: circular ring slot, dual slot, and quad slot. Finally, the quad slot discone antenna was considered to have advantages than any other types of antenna. This study shows the slot on the disc has an influence on the antenna performance, and by adjusting the shapes and position of the slot we could control the reflect coefficients and the radiation patterns of the antenna.

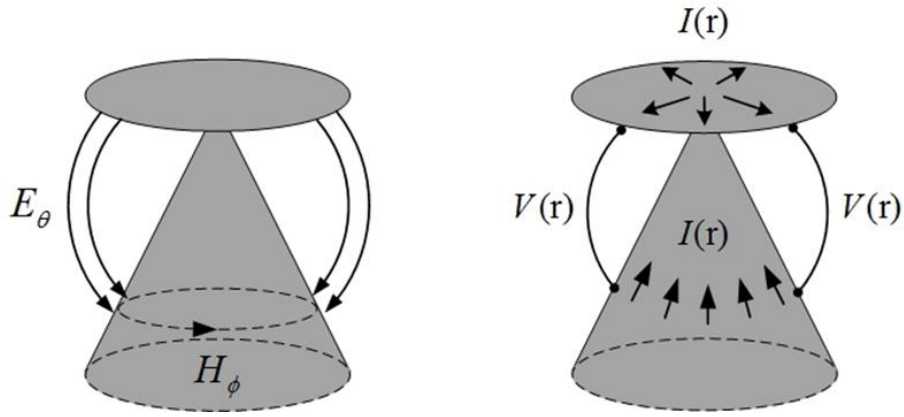


Figure 4.1 Electric and magnetic fields, and associated voltages and currents, for a disccone antenna

From Figure 4.1 we can observe the current distribution of the disccone antenna. The current distribution on antenna is a very important property, through the complete description of its amplitude and phase we can calculate the radiation pattern [39].

The disc of disccone antenna has circular shape, it offers better radiating properties compare to other shapes.

4.2 Study of Circular Ring Slot Architecture

The inspiration of circular ring slot architecture comes from [37], in which a circular ring slot antenna were proposed. Such slot antenna has simple geometry and symmetrical structure, when applied on the disccone antenna, it could create symmetrical radiation patterns. The proposed slot architecture is shown in Figure 4.2.

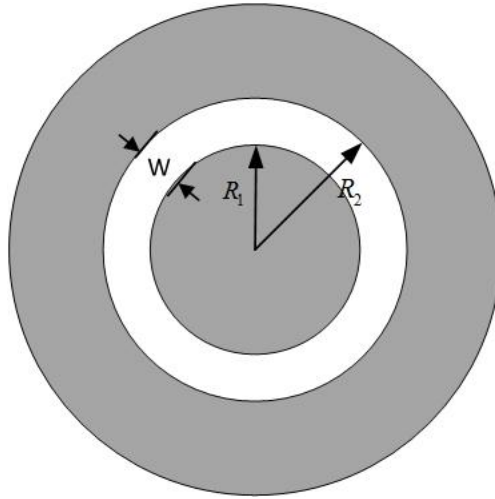


Figure 4.2 The circular ring slot architecture

For circular ring slot patch antenna we have [37]

$$f_a \approx \frac{c}{\pi(R_1 + R_2)} \times \sqrt{\frac{1 + \epsilon_r}{2\epsilon_r}} \quad (4-1)$$

f_a is the resonant frequency of the circular ring slot patch antenna.

ϵ_r is the relative permittivity of the dielectric material.

$\pi(R_1 + R_2)$ is the mean circumferences of the circular ring slot antenna.

To let the antenna resonate at frequency $f_a = 5.5GHz$, $\epsilon_r = 4.4$ then we have

$$\pi(R_1 + R_2) = 42.73mm$$

The slot radius is within the dimensions of disc, so the size of this proposed slot architecture is tolerable for the project.

The optimization values for the slot inner radius R_1 we choose are:

$$R_1 \in \{4, 6, 8, 10, 12\} \text{ mm}$$

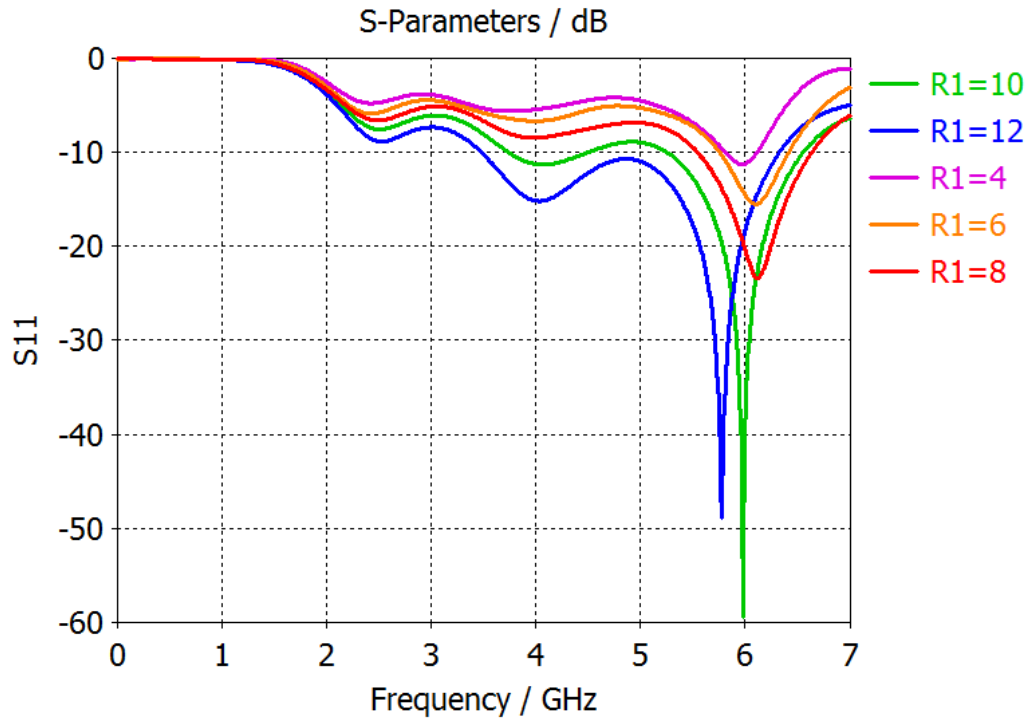


Figure 4.3 Variation of reflection coefficients with slot radius R_1

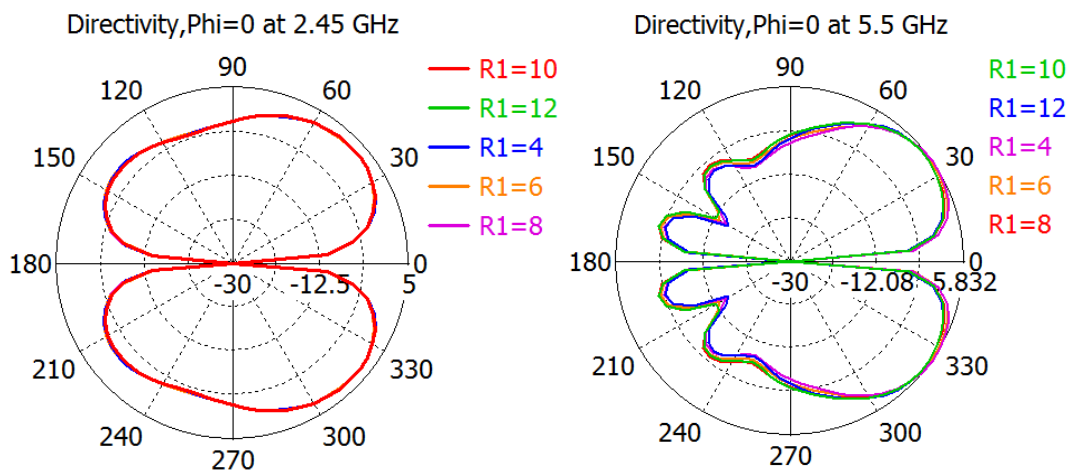


Figure 4.4 Variation of radiation patterns with slot radius at 2.45 GHz and 5.5 GHz

According to Figure 4.3, we can find the slot radius has a great influence on the reflection coefficients. For the radius smaller than 8 mm, the result is intolerable. Figure 4.4 shows the slot radius does not have much influence on the antenna radiation patterns. In order to have better view, we fix the result $R_1 = 12$ mm, and investigate the effect of slot width.

The optimization value for the slot inner radius W we choose are:

$$W \in \{1, 2, 3, 4, 5\} \text{ mm}$$

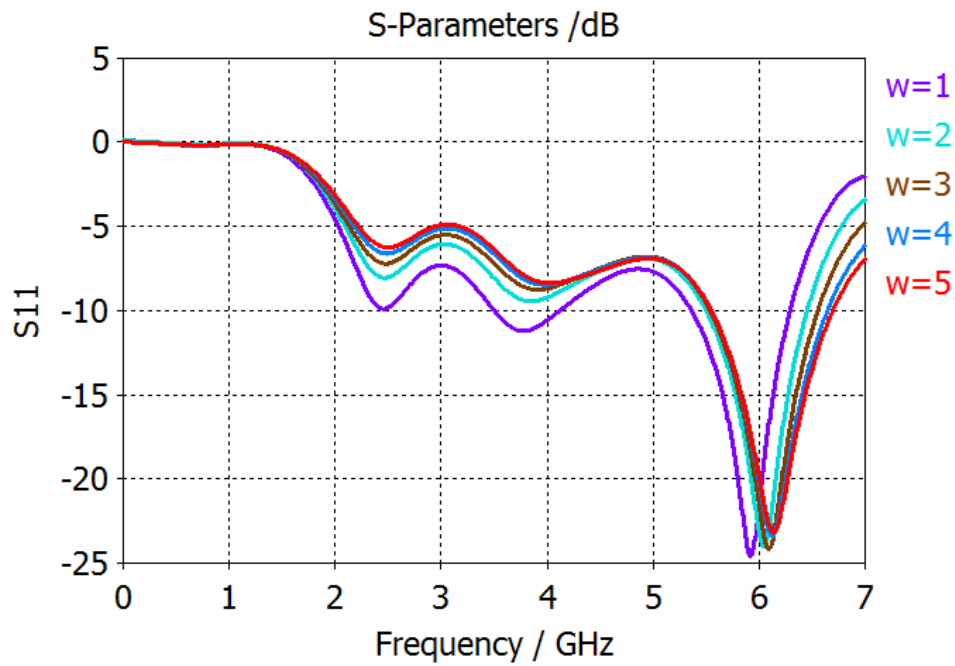


Figure 4.5 Variation of reflection coefficients with slot width

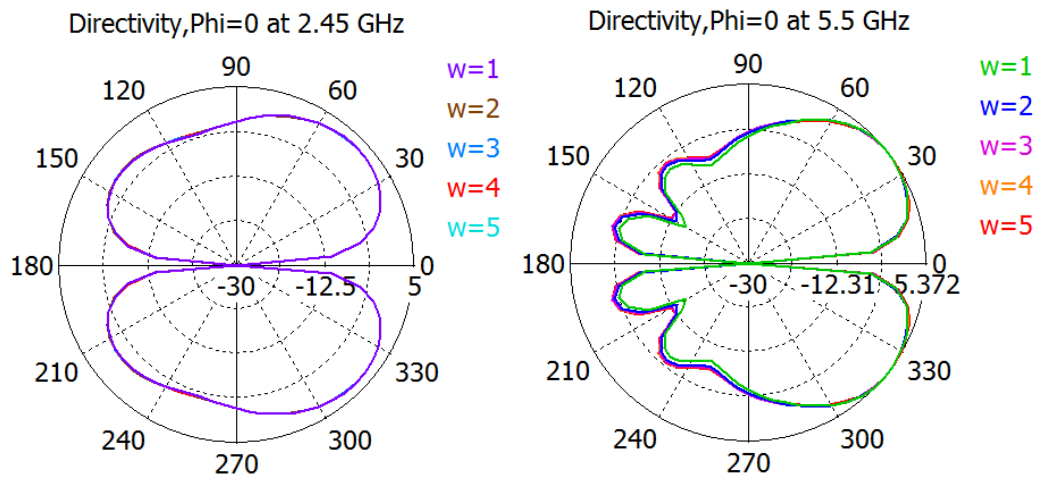


Figure 4.6 Variation of radiation patterns with slot width at 2.45 GHz and 5.5 GHz

By observing the reflection coefficients of different slot width from Figure 4.5, we can find when the width is larger than 3mm, the results are unacceptable. Besides, according to Figure 4.6, we can find the variation of the slot width did not have much influence on the antenna radiation patterns at both frequencies.

As a consequence, we find out this type of slot only suitable for the single band applications, it does not have satisfied performance for dual band applications, so we need to investigate for other slot architectures.

4.3 Study of Dual Slot Architecture

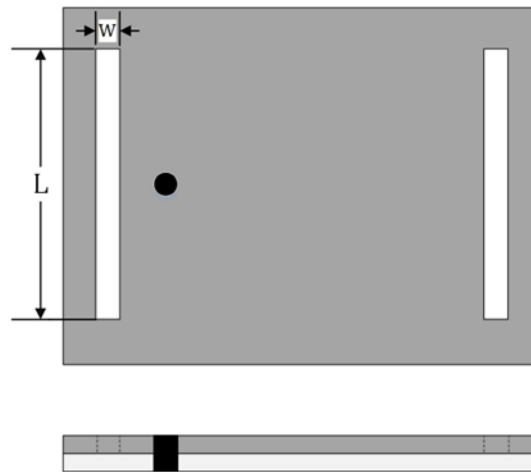


Figure 4.7 Slot-loaded rectangular patch

There are plenty of methods to achieve dual band operation, [38] introduced a type of slot architecture: two slots are located symmetrically at the edge of rectangular patch to achieve dual band operation, see Figure 4.7. These types of slots can change the current paths on the radiators; separate the radiator into more than one resonant region for multi-band operation. The length of the slot has an effect on the current flow along the slot. As the length increases, the resonant frequency increases.

In this project, since the disc is circular shape, two arc slots were carved on the disc instead of straight slot. The design of proposed antenna slot is shown in in Figure 4.8.

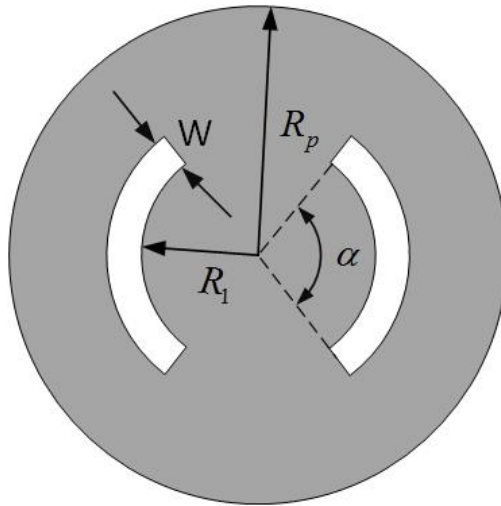


Figure 4.8 The dual slot architecture

In this section we need to optimise the slot length and width to obtain best antenna performance.

The optimization values for the slot inner radius R_1 we choose are:

$$R_1 \in \{5, 7, 9, 11, 13\} \text{ mm}$$

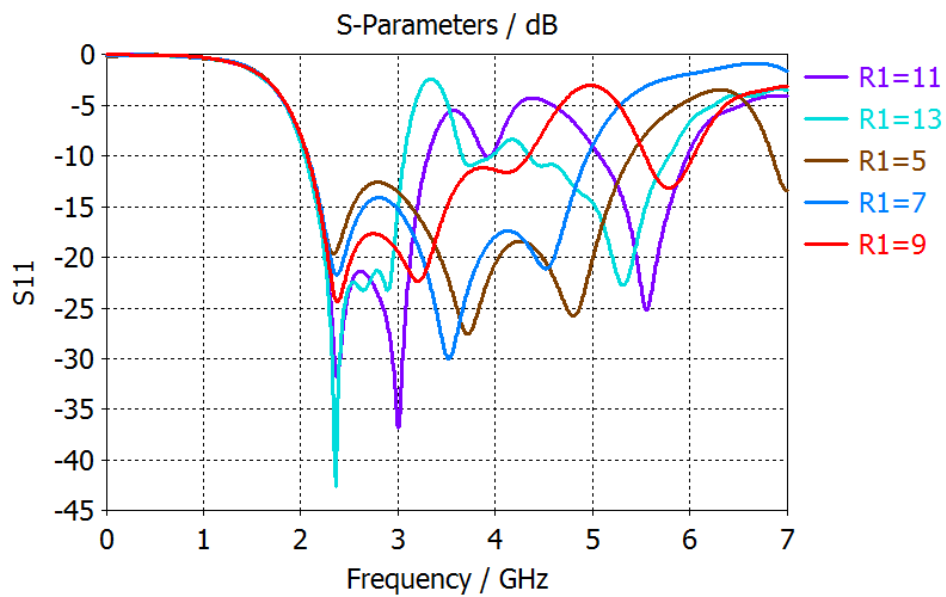


Figure 4.9 Variation of reflection coefficients with slot radius R_1

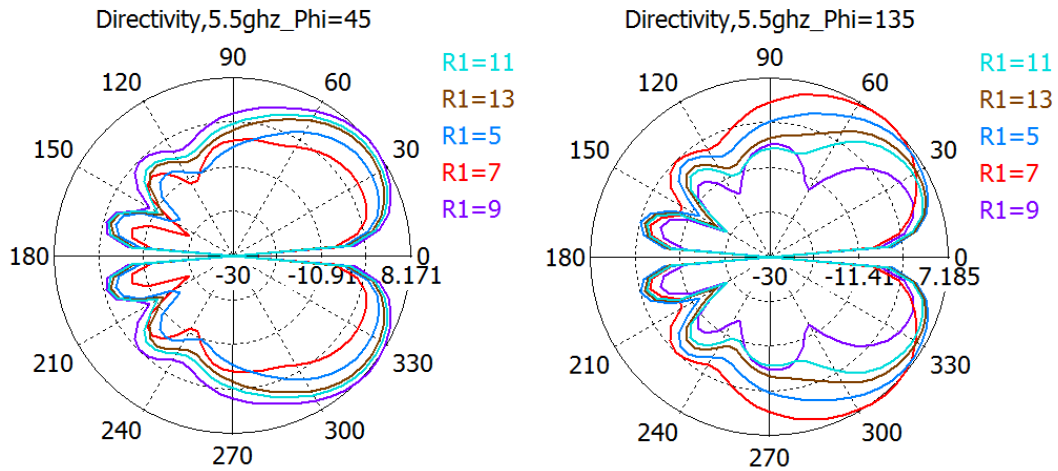


Figure 4.10 Variation of radiation patterns with slot radius R_1 at 5.5 GHz

Figure 4.9 and Figure 4.10 shows the slot length has great influence on the antenna reflect coefficients and radiation patterns, we can find when $R_1 = 11$ mm, the antenna reflection coefficient has the best performance. Fixing the slot radius $R_1 = 11$ mm, we then optimize the slot arc angle α .

The slot arc angle α is also the parameter which will influence the slot length.

The optimization values for the slot arc angle we choose are:

$$\alpha \in \{60, 70, 80, 90, 100\} \text{ deg}$$

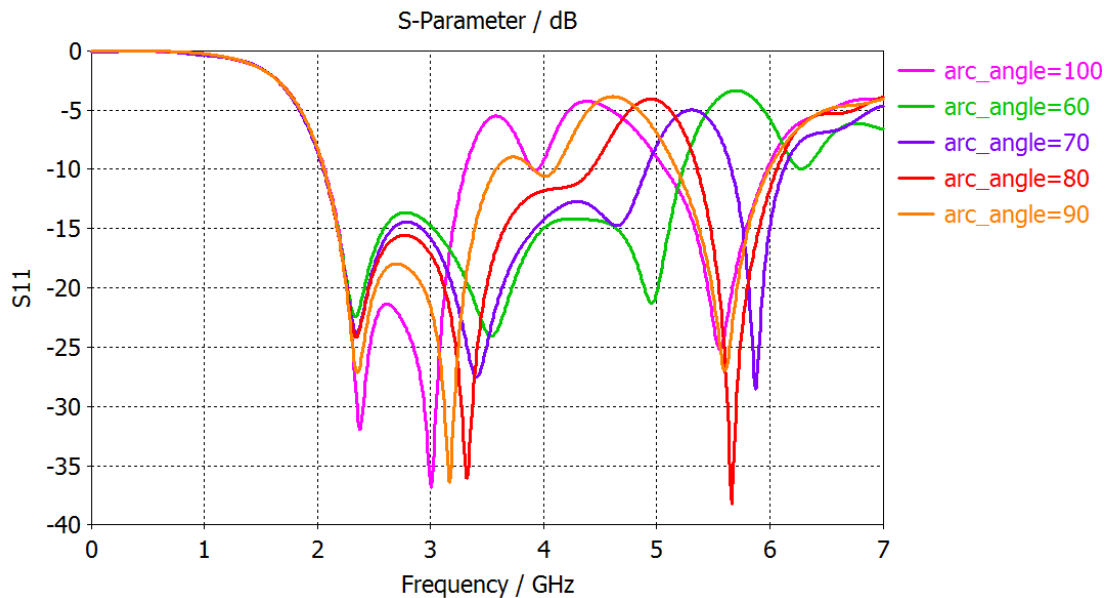


Figure 4.11 Variation of reflection coefficients with slot arc angle α

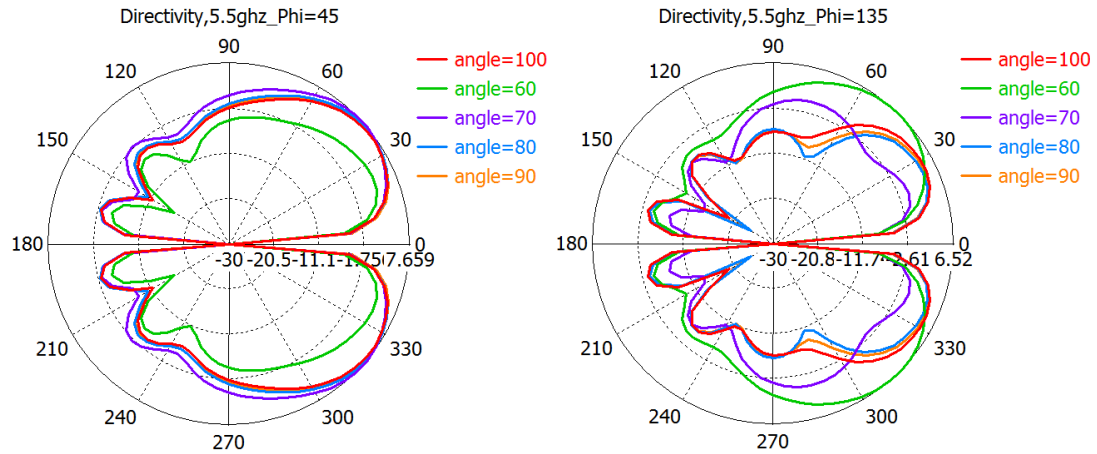


Figure 4.12 Variation of radiation patterns with slot arc angle α at 5.5 GHz

Figure 4.11 and Figure 4.12 shows the variation of the slot angle has the similar effect as the variation of slot radius, it has a great influence on the antenna reflection coefficients and radiation patterns. We can find when arc angle $\alpha = 100^\circ$, antenna reflection coefficient has the best performance.

Fixing the slot radius $R_1 = 11$ mm, $\alpha = 100^\circ$, the mean slot length we calculated is 21.80 mm. The next step is to optimize the slot width w .

The optimization values for the slot inner radius W we choose are:

$$W \in \{1, 2, 3, 4, 5\} \text{ mm}$$

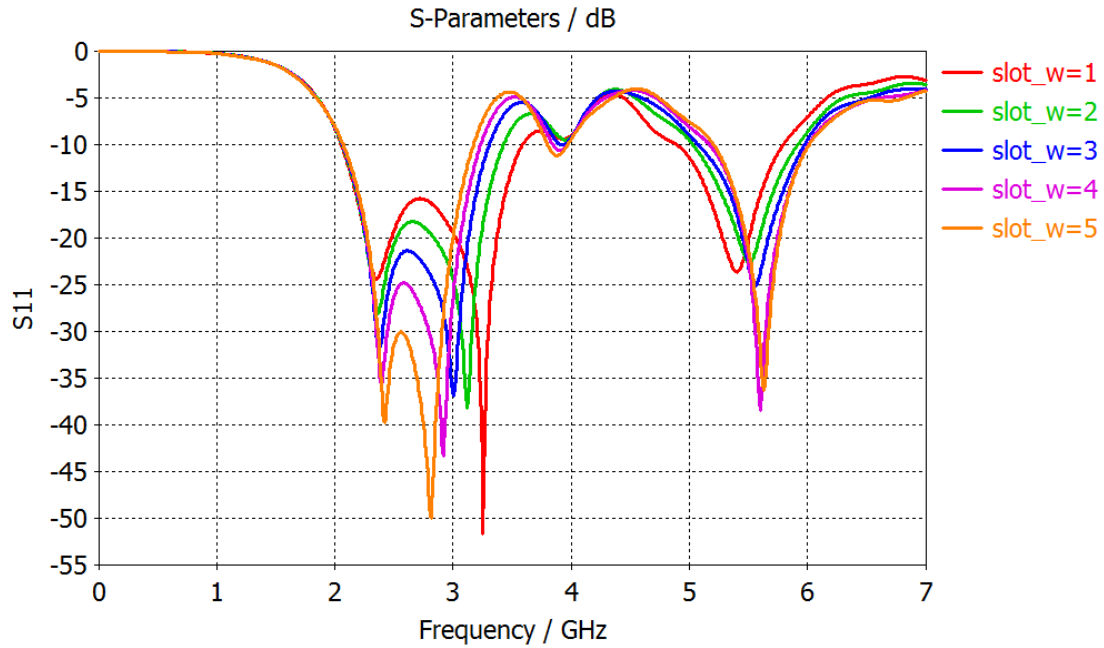


Figure 4.13 Variation of reflection coefficients with slot width

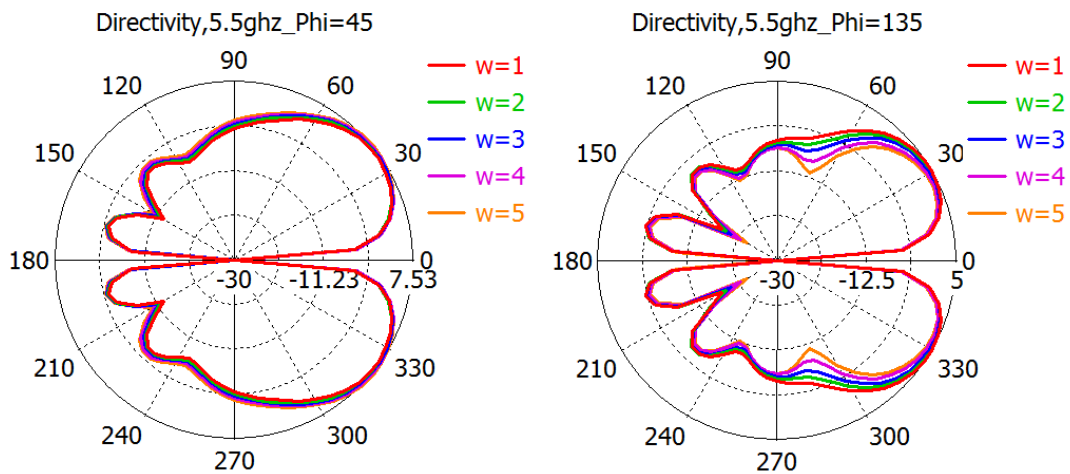


Figure 4.14 Variation of radiation patterns with slot width at 5.5 GHz

Figure 4.13 and Figure 4.14 shows the influence on antenna reflection coefficients and radiation patterns as slot width changes. It is found that the slot length has a great influence on the antenna radiation patterns, yet the slot width does not have much influence on the patterns. According to the observations, we can find the antenna has best performance when slot width $w=3$ mm. In Figure 4.15 shows the final optimum result.

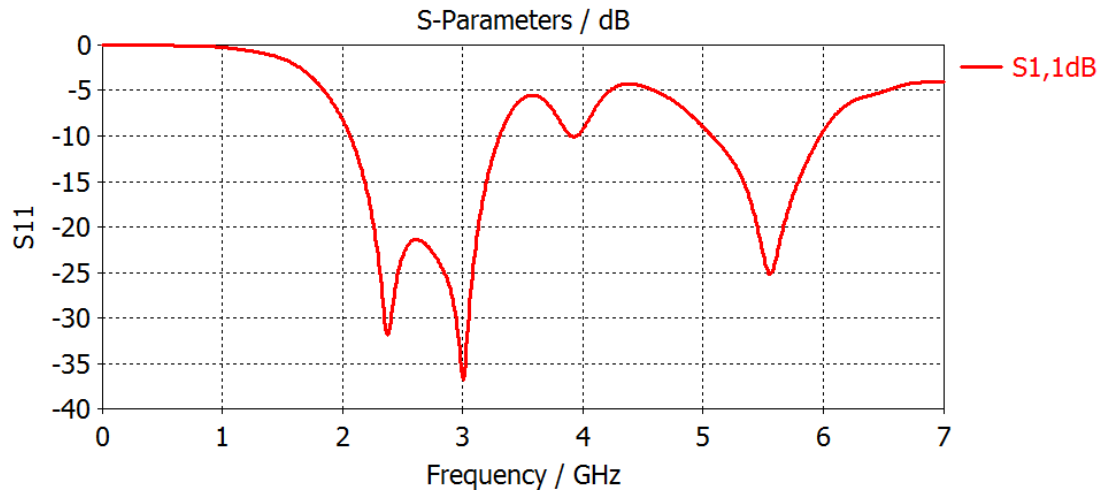


Figure 4.15 Optimum return loss

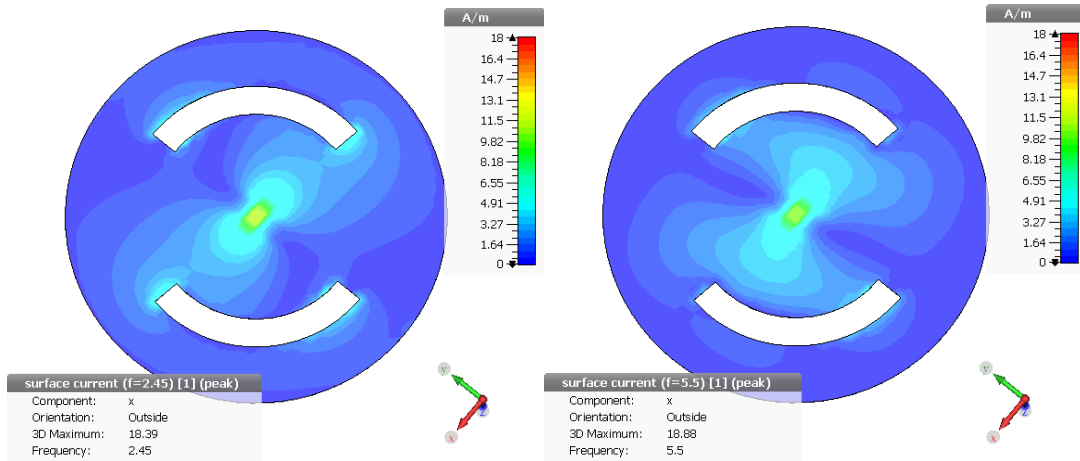


Figure 4.16 Surface current of disc

Figure 4.16 shows the surface current of the disc, since the disc is feeding from the back; the current is max at the feeding point. We can also observe the current flow around slot edge, from which the antenna radiates. The maximum current of 5.5 GHz is higher than 2.45 GHz, which result in higher gain [39].

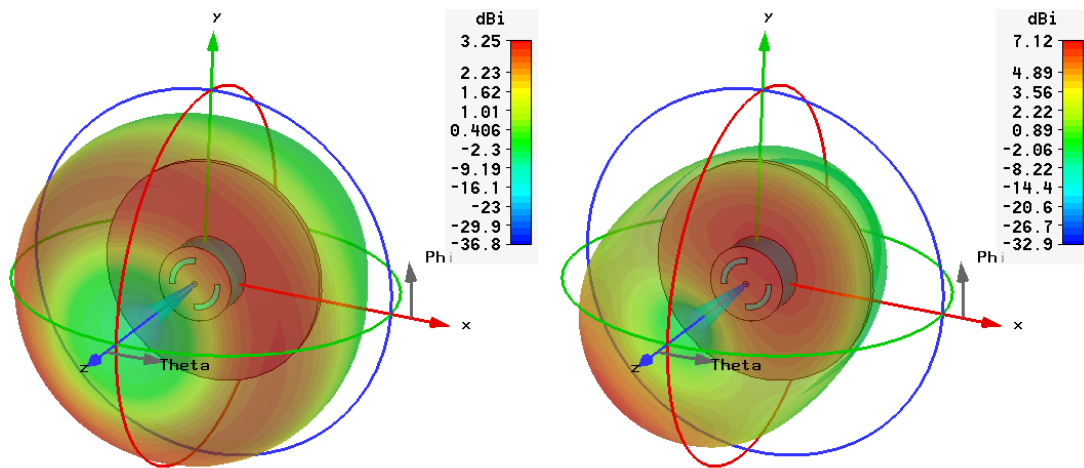


Figure 4.17 3D radiation patterns of the dual slot discone antenna

Although the reflection coefficient of this proposed dual slot discone antenna meet the requirement of our project, the maximum gain at both frequencies are much higher than other proposed structure, we can easily observe from Figure 4.17 that the radiation pattern is not omnidirectional at higher frequency. To obtain sufficient performance, we investigate third types of antenna: the quad slot discone antenna.

4.4 Study of Quad Slot Architecture

The performance of previous two slot architecture failed to meet the project requirements. In section 4.2 we can find if the slot architecture is not centrosymmetric geometry, the radiation pattern of antenna cannot be omnidirectional. As a result, in this section we proposed a quad slot disc antenna with centrosymmetric structure. Through the result, this antenna not only satisfied the project the requirements, it also has simple geometry which is ease of analysis and fabrication, the design of proposed antenna slot architecture is shown in Figure 4.18.

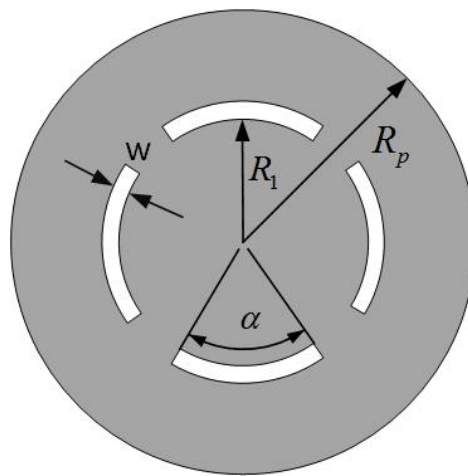


Figure 4.18 The quad slot architecture

The optimization steps are similar to the previous section; firstly we optimize the slot radius R_1 .

The optimization values for the slot inner radius R_1 we choose are:

$$R_1 \in \{4.5, 5.5, 6.5, 7.5, 8.5\} \text{ mm}$$

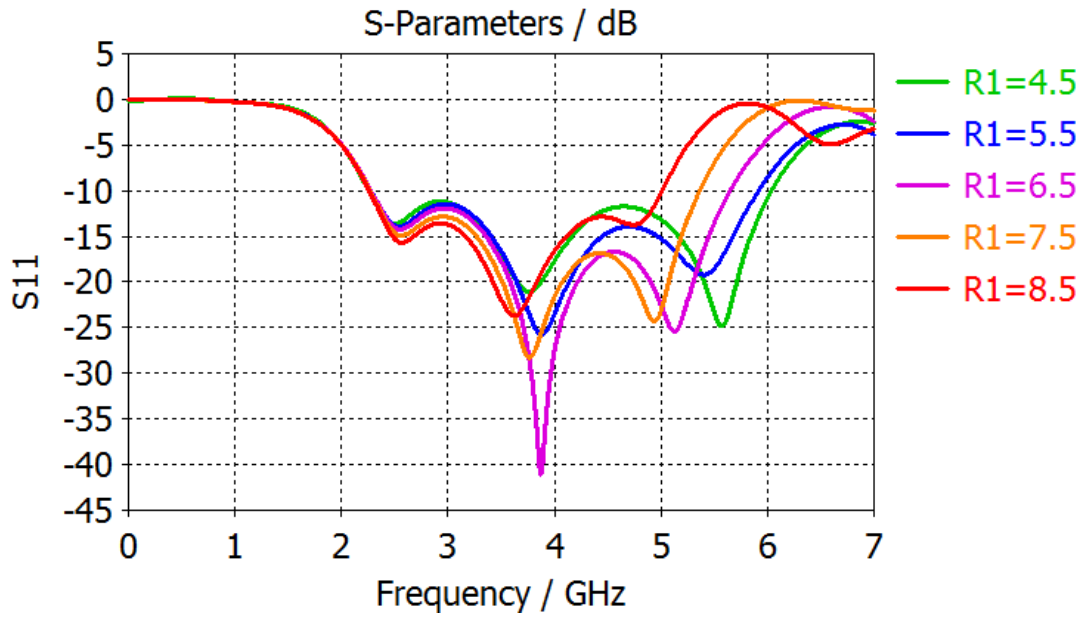


Figure 4.19 Variation of reflection coefficients with slot radius R_1

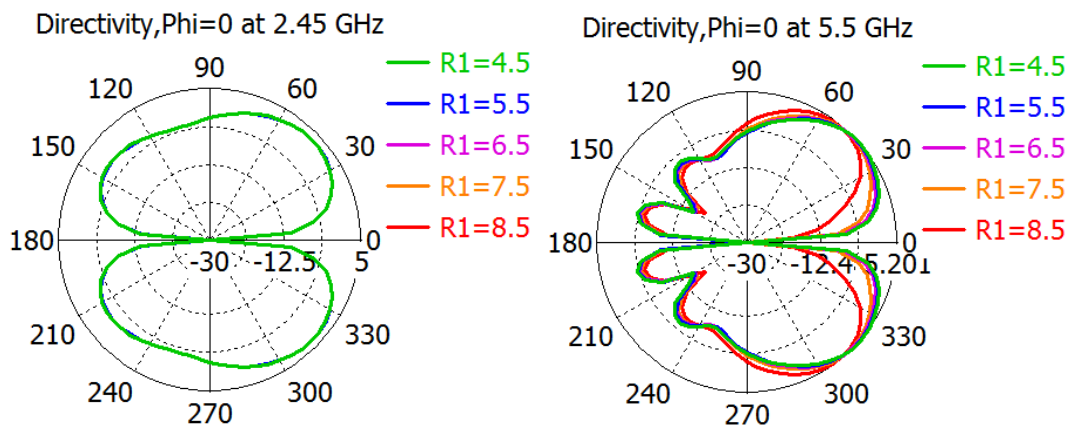


Figure 4.20 Variation of radiation patterns with slot radius R_1 at 2.45 GHz and 5.5 GHz

From Figure 4.19 and Figure 4.20, we can find the slot length has great influence on the antenna reflection coefficients and radiation patterns, when $R_1=8.5$ mm, the radiation pattern is the most desirable one, however, its reflection coefficient is unacceptable. To achieve better performance, we fixing the $R_1=6.5$ mm, the next step is to optimize the arc angle α . The slot arc angle α is also the parameter which will influence the slot length.

The optimization values for the slot arc angle we choose are:

$$\alpha \in \{65, 70, 75, 80, 85\} \text{ mm}$$

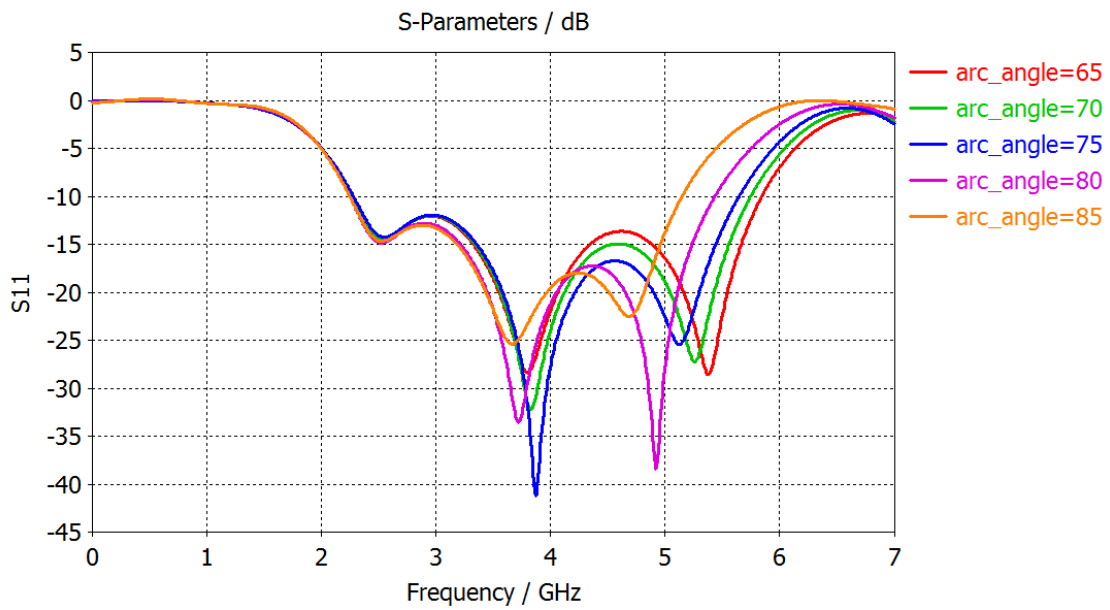


Figure 4.21 Variation of reflection coefficients with slot arc angle α

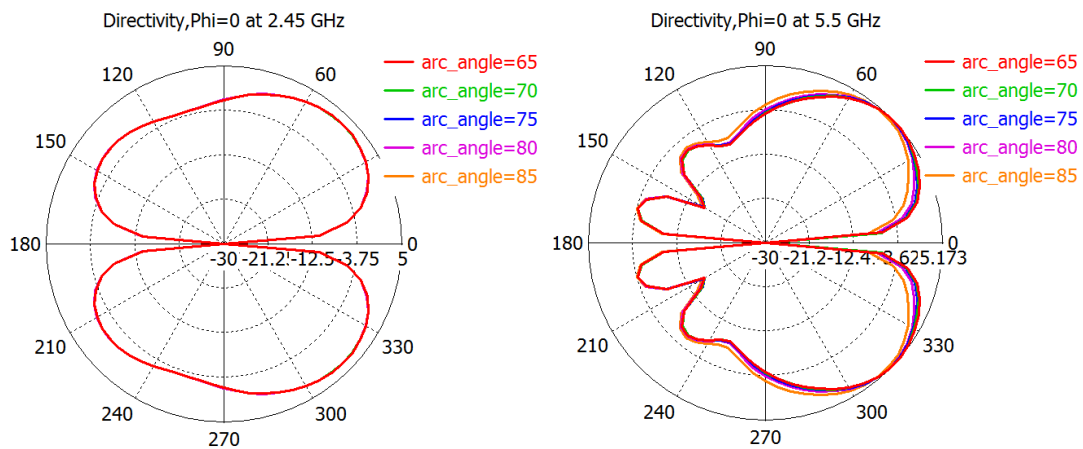


Figure 4.22 Variation of radiation patterns with slot arc angle α at 2.45 GHz and 5.5 GHz

From Figure 4.21 and Figure 4.22, we can find the variation of arc angle α has the same effect as the variation of slot radius R_1 . Fixing the arc angle $\alpha=75$ deg, the next step is to optimize the slot width W .

The optimization values for the slot width W we choose are:

$$W \in \{1, 2, 3, 4, 5\} \text{ mm}$$

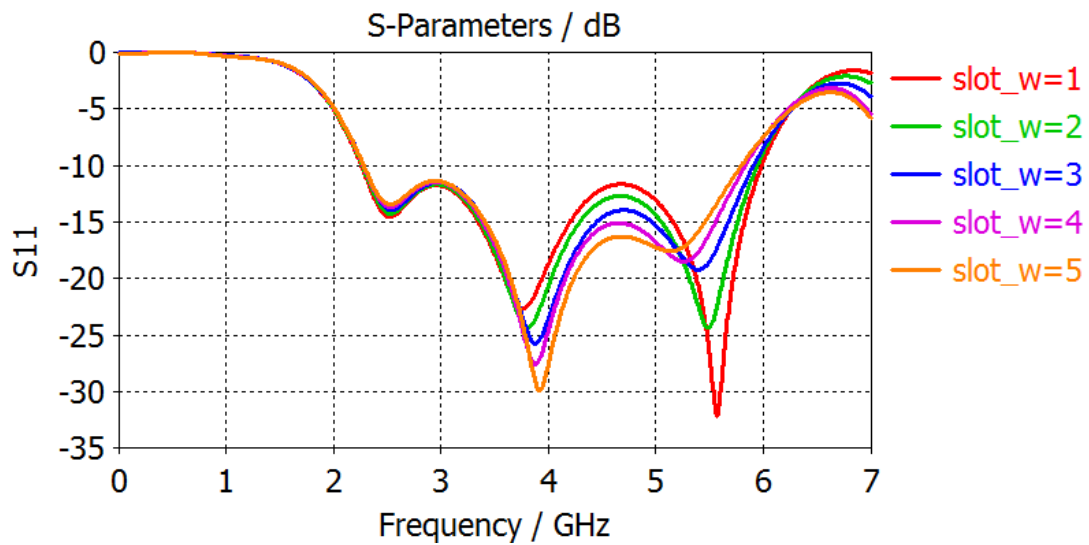


Figure 4.23 Variation of reflection coefficients with slot width W

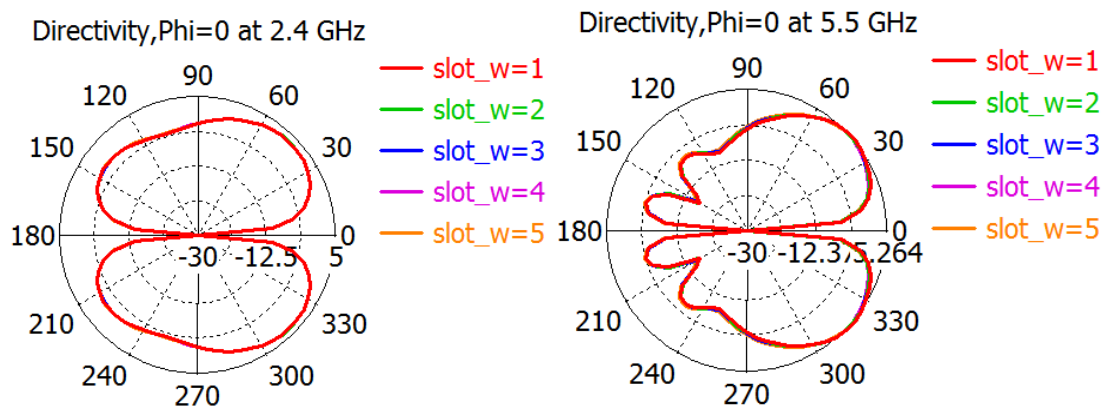


Figure 4.24 Variation of radiation patterns with slot width W at 2.45 GHz and 5.5 GHz

From Figure 4.23 and Figure 4.24 we can observe the slot width did not have much influence on the antenna radiation patterns, yet when $W=1$, the reflection coefficient has the best performance.

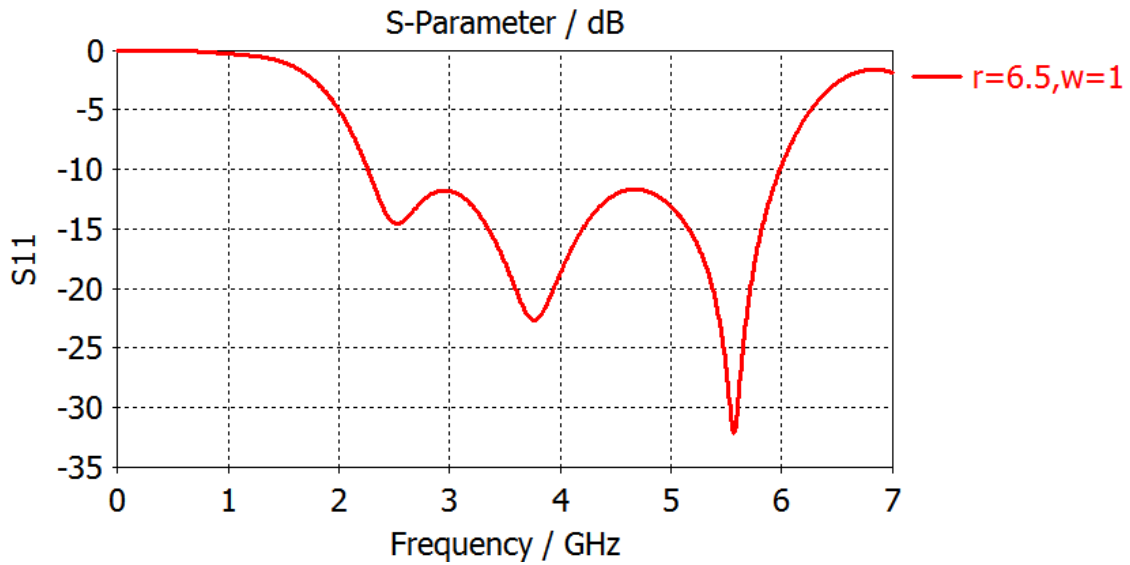


Figure 4.25 S11 parameters of the final design

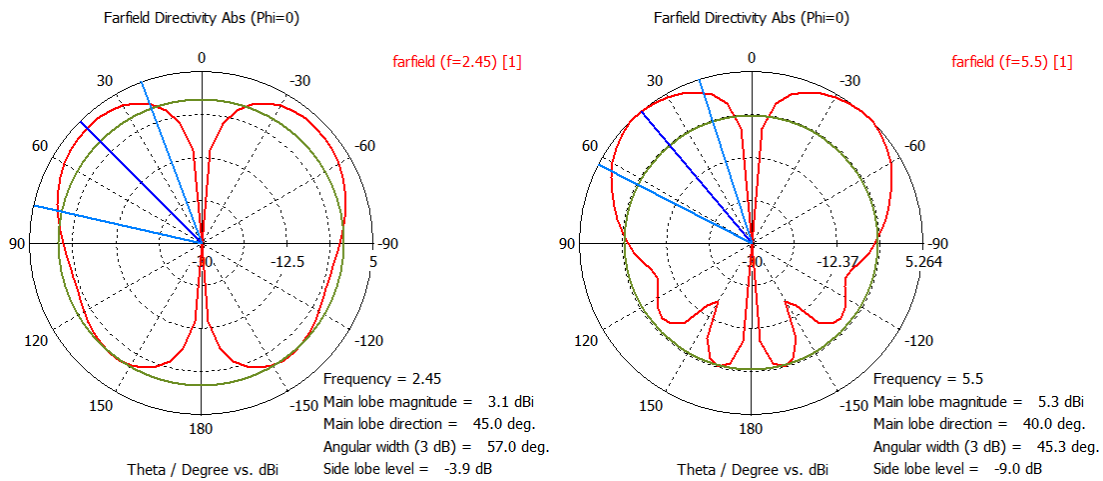


Figure 4.26 Radiation patterns of final design at 2.45GHz and 5.5 GHz

The final S11 result and radiation patterns at two working frequencies are shown in Figure 4.25, Figure 4.26, respectively. We can see from the figure that the impedance bandwidth of the antenna is from 2.25 GHz to 6 GHz, which is sufficient to cover the required bandwidth of project. The directivity of antenna is 3.1 dBi at 2.45 GHz and 5.3 dBi at 5.5 GHz. The radiation patterns are similar conical patterns at both working frequencies. The main lobe width of 40 deg at 5.5 GHz also increases compared with the discone antenna without slot.

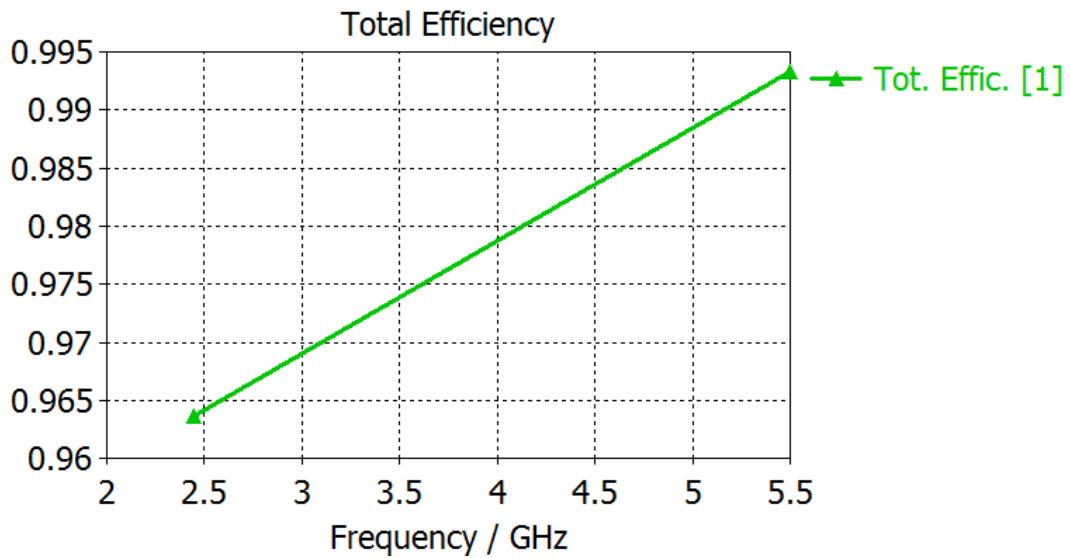


Figure 4.27 Total efficiency of the antenna

The total efficiency of this antenna is above 96%, which is much higher than the require 85% efficiency.

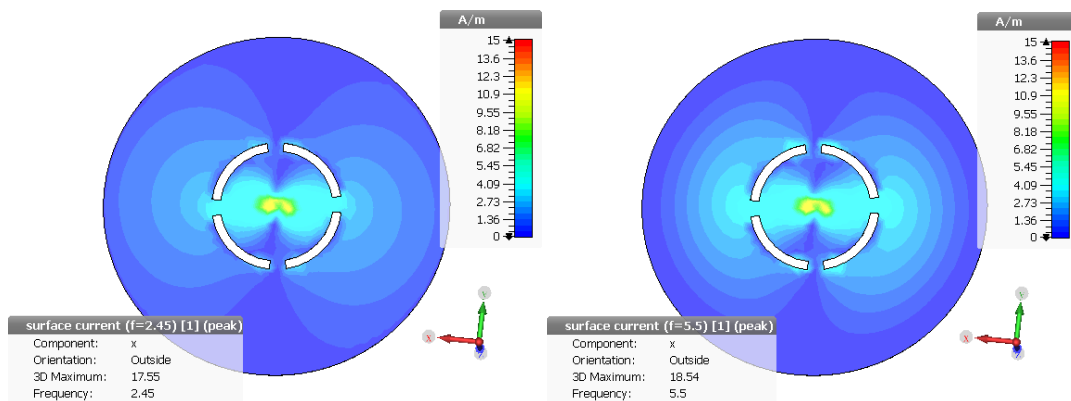


Figure 4.28 Surface current of disc

Figure 4.28 shows the surface current of the disc, since the disc is feeding from the back; the current is max at the feeding point. We can also observe the current flow around slot edge, from which the antenna radiates. The maximum current of 5.5 GHz is higher than 2.45 GHz, which results in higher gain [39].

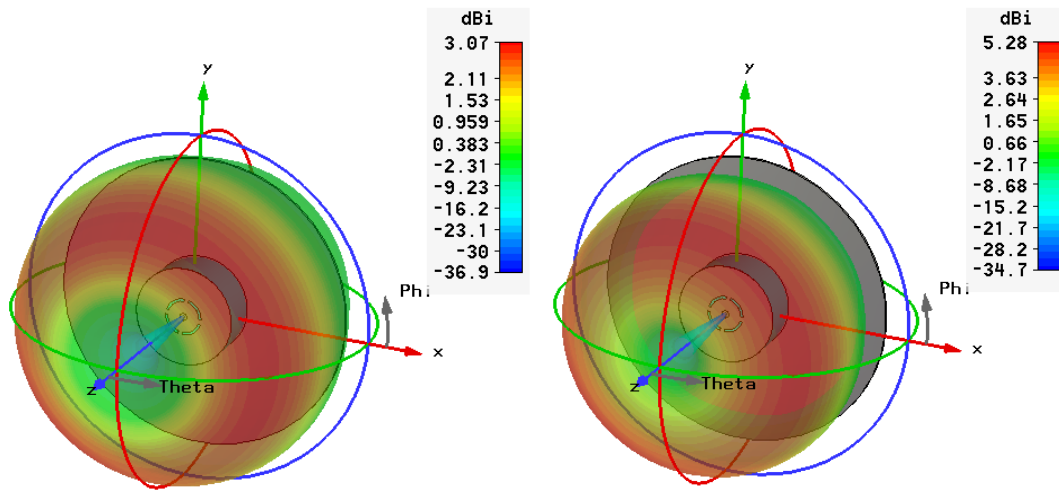


Figure 4.29 3D radiation patterns of the quad slot discone antenna

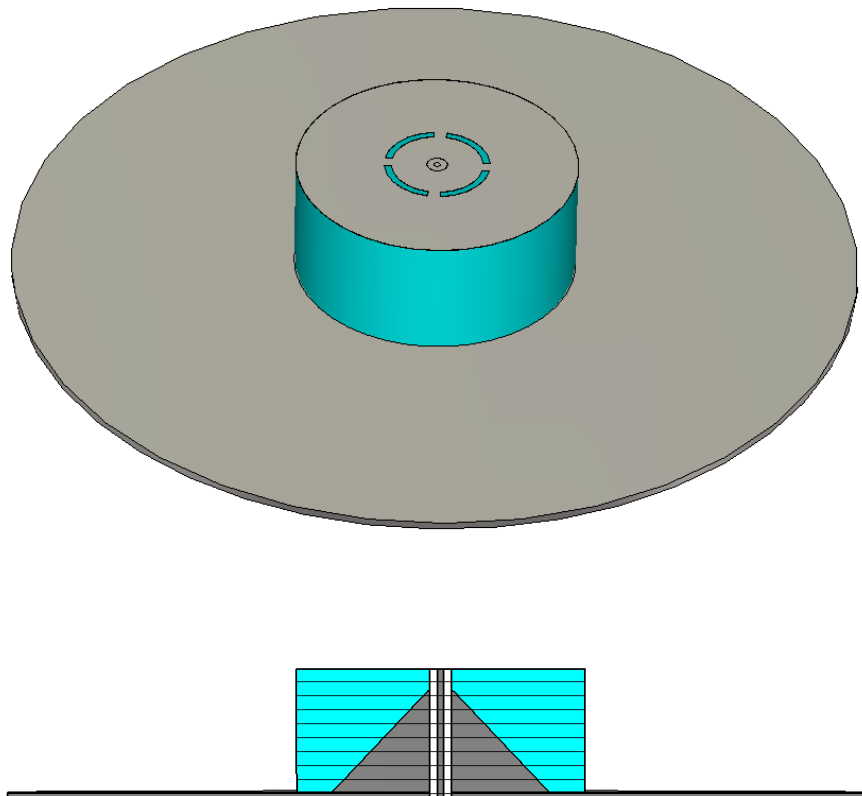


Figure 4.30 Final configuration of quad slot discone antenna

The 3D radiation patterns are shown in Figure 4.29, we can find that the radiation patterns of two working frequencies are two similar conical patterns. The final configuration of this discone antenna is shown in Figure 4.30. The antenna dimensions are 20 mm ×20 mm×18.5 mm which

located on a metallic ground plane with 1 mm thickness and 60 mm radius. This antenna dimensions is very compact within the project requirements. The parameters of final design are shown in Table 4.1.

Table 4.1 Parameters of final design

Parameters	Descriptions	Optimization start value
R_1	Slot radius	6.5 mm
w	Slot width	1 mm
α	Slot angle	75°
R_d	Radius of dielectric material	20 mm (fixed)
h_d	Discone overall height	17 mm
t_p	Thickness of disc	0.035 mm (fixed)
R_p	Radius of disc	20 mm
D_{up}	Upper cone diameter	3.47 mm (fixed)
R_c	Radius of cone	15 mm
h_c	Height of cone	14 mm
R_g	Radius of ground plane	60 mm
t_g	Thickness of ground plane	1 mm (fixed)
D_f	Diameter of feeding coax line	2.97 mm (fixed)
d_f	Diameter of feeding coax pin	0.91 mm (fixed)

5 Conclusions and Recommendations

Conclusions

In this thesis a transmitter antenna for WLAN applications to operate in both WLAN bands has been designed.

In order to achieve the desired performance, six different type of antennas suit for WLAN applications were carefully investigated. This study helps with providing the overview of advantages and disadvantages of different WLAN antennas. We found that the discone antenna has better performance over other antennas in terms of the impedance bandwidth, gain, and radiation patterns. In order to decrease dimensions and improve mechanical stability the discone antenna has been filled with dielectric.

This novel dielectric filled discone antenna overcomes the disadvantages of traditional discone, such as large dimensions, heavy weight. However, the performance of dielectric filled discone antenna without slot loading technique is not sufficient for the thesis requirements. As a result, in chapter 4 we proposed 3 types of slot architectures to make improvements on antenna's impedance bandwidth, radiation patterns, and gain. Through the study of three slot architectures, it is found that quad- slot architecture has advantages over other architectures. It satisfies the requirements of the project in terms of the dimensions, operational bandwidth, gain, and radiation patterns. This antenna has 3.75 GHz operational bandwidth (2.25-6.0 GHz) which covers all the main protocols of IEEE 802.11 a/g/b/n.

The proposed discone antenna achieves the omnidirectional radiation pattern at the azimuth plane and conical radiation pattern at the elevation plane. The radiation patterns are two similar conical patterns at 2.45 GHz and 5.5 GHz. Besides, the directivities at both working frequencies are 3.1 dBi at 2.45 GHz and 5.3 dBi at 5.5 GHz, which is much higher than the conventional WLAN dipole antennas.

The drawback of this antenna is the cost of fabrication which is relatively higher than other conventional printed narrowband antennas. However, the outstanding performance of this antenna like radiating properties, broadband operation cannot be replaced by other conventional antennas. This is the trade-off we have to make between manufacture cost and antenna performance.

Recommendations for the future

The specifications of this thesis are quite ambitious, through the performance of this discone antenna has already met the requirements of the project, it has not reached its limit yet, the impedance bandwidth and gain still has room for the future improvement.

Due to its discone architecture, this antenna has great potential for broadband applications. In chapter 4, we investigate the slot effect on antennas impedance bandwidths, radiation patterns, antenna gain at 2.4 GHz and 5.5 GHz. However, by making novel slot architecture on the disc of the antenna, it is possible to make it suitable for triple or even quad-bandwidths applications.

Appendix A

The filled in dielectric material we used in this project is Preperm® L440 [40], it can be processing in the following processing conditions:

Table. A Processing conditions of Preperm® L440

Injection moulding	
Material temperature	290-310°C
Mould temperature	80-140°C
Injection pressure	600-800 bar
Injection speed	moderate

The characteristic of Preperm® L440 is present in the table below.

Table. B Characteristics of Preperm® L440

Typical Properties of Preperm® L440	
Physical Properties	
Specific gravity (g/cm ³)	1.54
Tensile strength (MPa)	46
Yield strength (MPa)	52
Elongation at break	30 %
Elongation at yield	8 %
Mould shrinkage	0.8 %
Melt Flow Index	
300°C/2.16 kg	20
300°C/5.0 kg	60
Electrical Properties	
Dissipation factor (1 GHz)	0.0005
Dielectric constant (1 GHz)	4.4

Appendix B

Table. C Characteristics of RG402/U

Typical Properties of RG402/U	
Physical specifications	
Operating temperature	-55 to +125 degree
Inner conductor	
Material	Copper Clad Steel
Plating	Silver
Diameter (mm)	0.91
Dielectric	
Material	Polytetrafluoroethylene (PTFE)
Diameter (mm)	2.97
Shield	
Material	Copper
Diameter (mm)	3.58
Jacket	
one time minimum bend diameter (mm)	3.81
Electric specifications	
Impedance (Ohms)	50
Maximum operational frequency (GHz)	36
Capacitance (pF/ft)	29.9
Dielectric material permittivity (F/m)	1.99
Dielectric material $\tan\delta$	0.0004

Acknowledgements

Ever since the first day I came to Netherlands, many people have helped me. I would like to say thanks to all of you in here, though words are not enough to express my gratitude.

First of all, I would like to express my sincere thanks to my responsible professor Prof. DSc. Alexander Yarovoy, who provides me the chance to start my thesis in Microwave Sensing, Signals and Systems (MS3) group. In 2013 I made my decision came to MS3 group to do my thesis because of your patience and extensive knowledge I felt during the course. I have been receiving advices and encouragements from you on my work constantly and they give me the courage to keep on going.

I would like to say I own a lot to my daily supervisor: Ir. Dinh Tran, this thesis would not have been possible without the help from you. I appreciated your patient response and detailed feedbacks on every piece of my text, and thank you for the advice and instructions during our numerous meetings. Moreover, I am impressed by your sparking ideas and passionate in antennas.

Besides my responsible professor and daily supervisors, I would like to thank committee member Dr.ir. Gerard Janssen, thanks a lot for your time spent on this thesis and your valuable feedback.

I would like to say thank you to my colleagues from MS3 group Shilong Sun and Jianping Wang for the kind suggestions on my study.

I want to say thank you to all my friends, your accompany fulfilled my life. In a place where thousand miles always from home, we are like brothers and sisters, I will never forget the precious time we spend together.

Finally, I want to express my deep love to my parents, without your unconditional love and support I could never make it today. I have always felt lucky to have wonderful parents like you, who understand me so much.

Bibliography

- [1] IEEE Standards Association. "802.11-2012-IEEE Standard for Information technology–Telecommunications and information exchange between systems Local and metropolitan area networks–Specific requirements Part 11: Wireless LAN Medium Access Control (MAC) and Physical Layer (PHY) Specifications." (2012).
- [2] Goldsmith, Andrea. *Wireless communications*. Cambridge university press, 2005.
- [3] litepoint.com, (2013). *IEEE 802.11ac: What Does it Mean for Test?*. [online] Available at: http://litepoint.com/whitepaper/80211ac_Whitepaper.pdf [Accessed 22 Apr. 2015].
- [4] Tran, D., et al. "Architecture and Design Procedure of a Generic SWB Antenna with Superb Performances for Tactical Commands and Ubiquitous Communications." (2012).
- [5] Kim, Ki-Hak, Jin-U. Kim, and Seong-Ook Park. "An ultrawide-band double disc antenna with the tapered cylindrical wires." *Antennas and Propagation, IEEE Transactions on* 53.10 (2005): 3403-3406.
- [6] Su, Saou - Wen. "Concurrent dual - band six - loop - antenna system with wide 3 - dB beamwidth radiation for MIMO access points." *Microwave and Optical Technology Letters* 52.6 (2010): 1253-1258.
- [7] Su, Saou-Wen. "Very-low-profile monopole antennas for concurrent 2.4-and 5-GHz WLAN access-point applications." *Microwave and Optical Technology Letters* 51.11 (2009): 2614-2617.
- [8] Chou, Jui-Hung, and Saou-Wen Su. "Internal wideband monopole antenna for MIMO access-point applications in the WLAN/WIMAX bands." *Microwave and Optical Technology Letters* 50.5 (2008): 1146-1148.
- [9] Cho, Young Jun, Yong Sun Shin, and Seong-Ook Park. "An internal PIFA for 2.4/5 GHz WLAN applications." *Microwave Conference Proceedings, 2005. APMC 2005. Asia-Pacific Conference Proceedings*. Vol. 4. IEEE, 2005.

- [10] Nashaat, Dalia Mohammed, Hala A. Elsadek, and Hani Ghali. "Single feed compact quad-band PIFA antenna for wireless communication applications." *Antennas and Propagation, IEEE Transactions on* 53.8 (2005): 2631-2635.
- [11] Huynh, M-C., and Warren Stutzman. "Ground plane effects on planar inverted-F antenna (PIFA) performance." *IEE Proceedings-Microwaves, Antennas and Propagation* 150.4 (2003): 209-213.
- [12] Abedin, M. F., and M. Ali. "Modifying the ground plane and its effect on planar inverted-F antennas (PIFAs) for mobile phone handsets." *Antennas and Wireless Propagation Letters, IEEE* 2.1 (2003): 226-229.
- [13] Chang, Chih-Hua, and Kin-Lu Wong. "Printed-PIFA for penta-band WWAN operation in the mobile phone." *Antennas and Propagation, IEEE Transactions on* 57.5 (2009): 1373-1381.
- [14] Luk, Kwai Man, and Kwok Wa Leung, eds. *Dielectric resonator antennas*. London: Research Studies Press, 2003.
- [15] Gao, Yuan, et al. "Dual-band hybrid antenna for wlan application." *Antennas and Propagation Society International Symposium 2006, IEEE*. IEEE, 2006.
- [16] Gao, Yuan, Ban-Leong Ooi, and Alexandre P. Popov. "Dual-band hybrid dielectric resonator antenna with CPW-fed slot." *Microwave and optical technology letters* 48.1 (2006): 170-172.
- [17] Rao, Qinjiang, et al. "Compact independent dual-band hybrid resonator antenna with multifunctional beams." *Antennas and Wireless Propagation Letters, IEEE* 5.1 (2006): 239-242.
- [18] Zhang, Zhijun, et al. "Dual-band WLAN dipole antenna using an internal matching circuit." *Antennas and Propagation, IEEE Transactions on* 53.5 (2005): 1813-1818.
- [19] Wu, Ya-Jie, et al. "Triple-band omni-directional antenna for WLAN application." *Progress In Electromagnetics Research* 76 (2007): 477-484.
- [20] Yeh, S. H., et al. "2.4/5.2 GHz Dual-WLAN unequal-arms dipole antenna with a chip inductor for omni-directional radiation patterns." *IEEE Region*. Vol. 10. 2007.

- [21] Wikipedia, (2015). *Dipole antenna*. [online] Available at: http://en.wikipedia.org/wiki/Dipole_antenna [Accessed 28 May 2015].
- [22] Qu, Shi-Wei, et al. "Wideband cavity-backed bow-tie antenna with pattern improvement." *Antennas and Propagation, IEEE Transactions on* 56.12 (2008): 3850-3854.
- [23] Qu, Shi-Wei, Chi-Hou Chan, and Quan Xue. "Ultrawideband composite cavity-backed folded sectorial bow-tie antenna with stable pattern and high gain." *Antennas and Propagation, IEEE Transactions on* 57.8 (2009): 2478-2483.
- [24] Black, D. N., and Theresa A. Brunasso. "An ultra-wideband bicone antenna." *Ultra-Wideband, The 2006 IEEE 2006 International Conference on*. IEEE, 2006.
- [25] Balanis, Constantine A. *Antenna theory: analysis and design*. John Wiley & Sons, 2012
- [26] Smith, P. Do P. "The conical dipole of wide angle." *Journal of Applied Physics* 19.1 (1948): 11-23.
- [27] Papas, Charles H., and Ronold King. "Input impedance of wide-angle conical antennas fed by a coaxial line." *Proceedings of the IRE* 37.11 (1949): 1269-1271.
- [28] Lu, Mingyu, et al. "Theoretical and experimental study of a quasi-planar conical antenna." *Antennas and Propagation Society International Symposium, 2007 IEEE*. IEEE, 2007.
- [29] Lu, Mingyu, et al. "A quasi-planar wide band conical antenna." *Ultra-Wideband Short-Pulse Electromagnetics 8*. Springer New York, 2007. 25-32.
- [30] Milligan, Thomas A. *Modern antenna design*. John Wiley & Sons, 2005.
- [31] Nagasawa, Koji, and Isamu Matsuzuka. "Radiation field consideration of biconical horn antenna with different flare angles." *Antennas and Propagation, IEEE Transactions on* 36.9 (1988): 1306-1310.
- [32] Pozar, David M. *Microwave engineering*. John Wiley & Sons, 2009.
- [33] Thiele, WL Stutzman GA, and Warren L. Stutzman. "Antenna theory and design." *Sections 7* (1981).
- [34] Pasternack.com, (2013). *RG402 Coax Cable with Copper Outer Conductor*. [online] Available at: <http://www.pasternack.com/images/ProductPDF/RG402-U.pdf> [Accessed 22 Apr. 2015].

- [35] Kim, Jinu, and Seong-Ook Park. "Novel ultra-wideband discone antenna." *Microwave and Optical Technology Letters* 42.2 (2004): 113-115.
- [36] Arslan, Huseyin, Zhi Ning Chen, and Maria-Gabriella Di Benedetto, eds. *Ultra wideband wireless communication*. John Wiley & Sons, 2006.
- [37] Wong, Kin-Lu, Chien-Chin Huang, and Wen-Shan Chen. "Printed ring slot antenna for circular polarization." *Antennas and Propagation, IEEE Transactions on* 50.1 (2002): 75-77.
- [38] See, T. S. P., and Zhi Ning Chen. "Slot-loaded center-fed microstrip patch antenna." *Microwave and Optical Technology Letters* 34.3 (2002): 227-232.
- [39] Silver, Samuel, ed. *Microwave antenna theory and design*. No. 19. Iet, 1949.
- [40] premixgroup.com, (n.d.). *PREPERM® L440*. [online] Available at: http://www.premixgroup.com/wp-content/uploads/2015/02/preperm_l440_tds.pdf [Accessed 22 Apr. 2015].